

Управление оптическими свойствами биологических тканей: новые приложения в мультимодальной визуализации и фототерапии

В.В. Тучин

Саратовский национальный исследовательский государственный университет им.
Н.Г. Чернышевского, Саратов

Национальный исследовательский Томский государственный университет, Томск
Институт проблем точной механики и управления РАН, Саратов

tuchinvv@mail.ru



Saratov State University & Saratov State Medical University

- ❖ Motivation and basics of tissue optical clearing
- ❖ Creation of UV window
- ❖ Fluorescence measurements
- ❖ Combined MRI and fluorescence imaging
- ❖ Practical examples, spectroscopy, imaging and treatment
- ❖ Summary
- ❖ Conclusion

Motivation: Challenges of Optical Imaging and Treatment



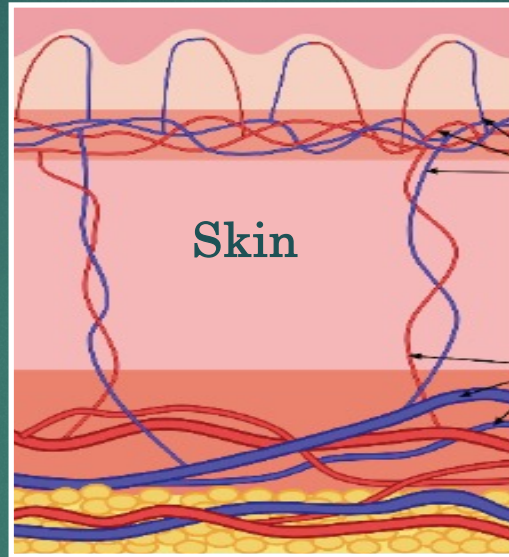
Soft limit $\sim \delta$

$$\delta = 1 / \sqrt{3\mu_a(\mu_a + \mu'_s)}$$

Hard limit $\sim 10\delta$

$$\text{MFP} = l_{ph} = 1 / (\mu_a + \mu_s)^{-1}$$

$$\mu'_s = \mu_s(1 - g)$$



OM, SNOM

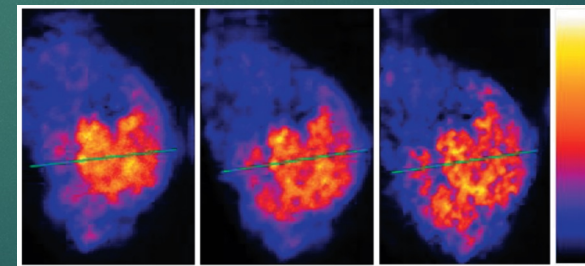
CFM, 2PM, SHM, etc.

OCT

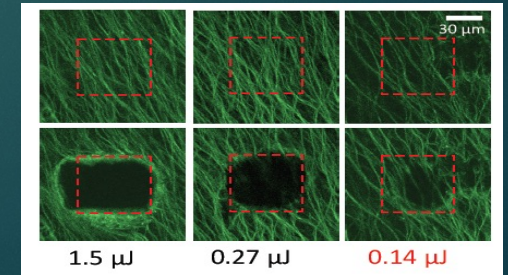
DOT, UOT, PAT

1 - 2 mm

- OM: Optical microscopy
- SNOM: Scanning near-field optical microscopy
- CFM: Confocal microscopy
- 2PM: Two-photon microscopy
- SHM: Second harmonic microscopy
- OCT: Optical coherence tomography
- DOT: Diffuse optical tomography
- UOT: Ultrasound-modulated optical tomography
- PAT: Photoacoustic tomography

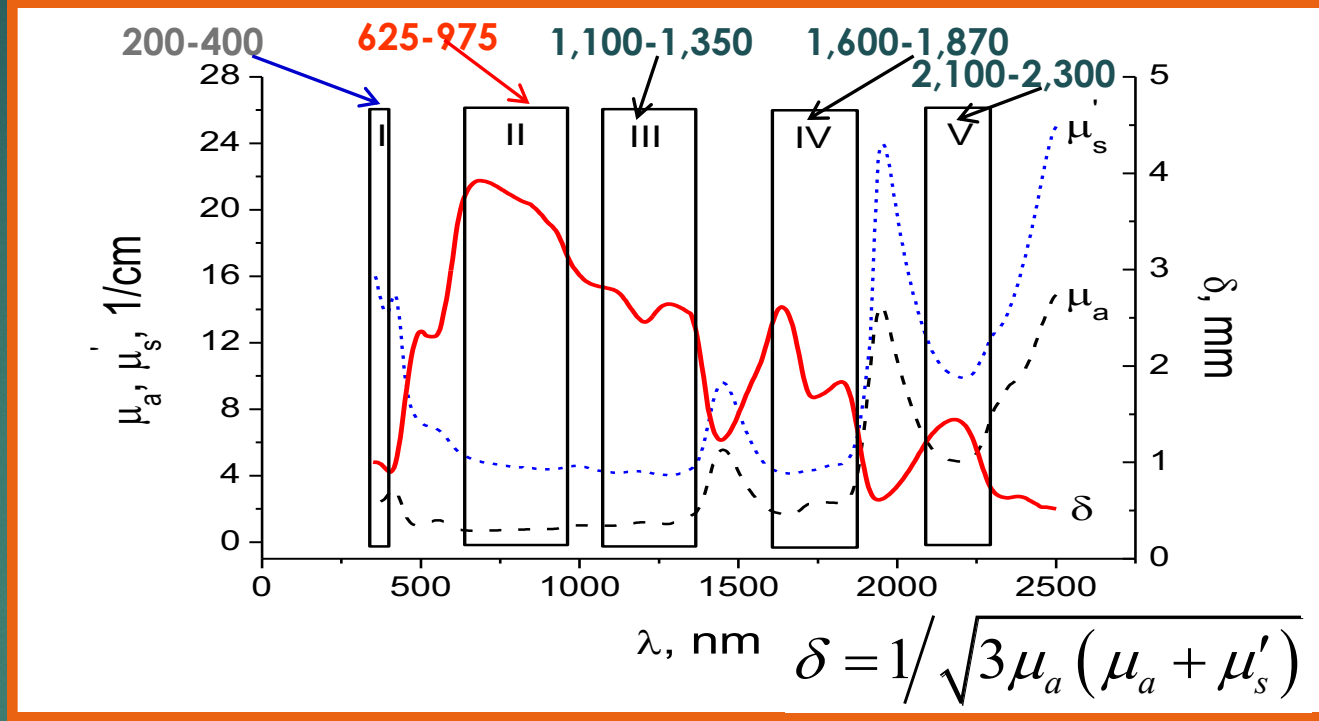
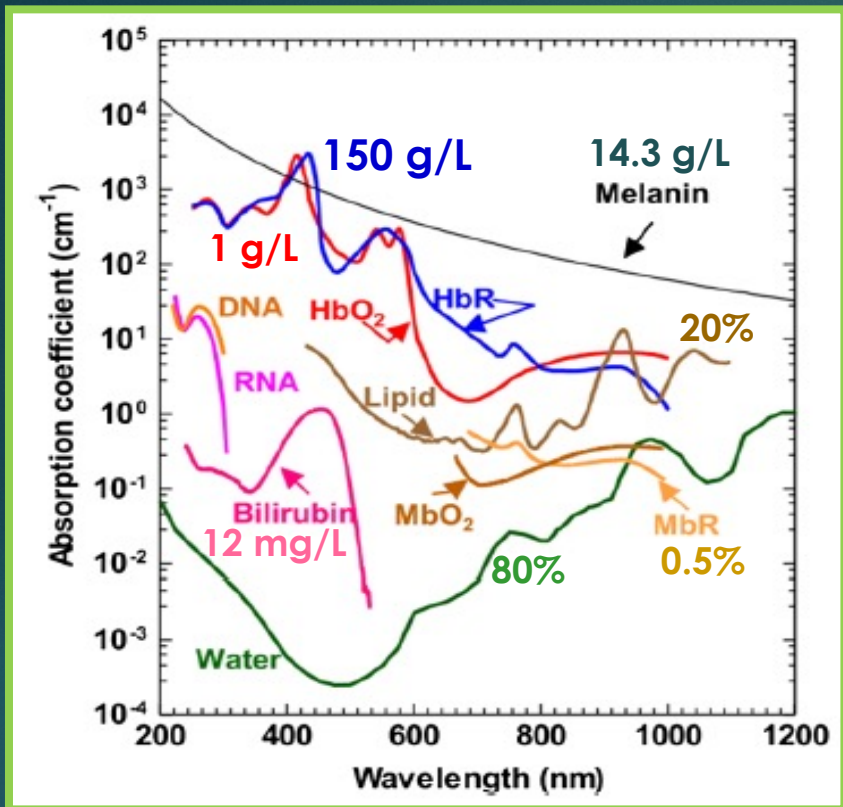


Fluorescence cancer cell imaging



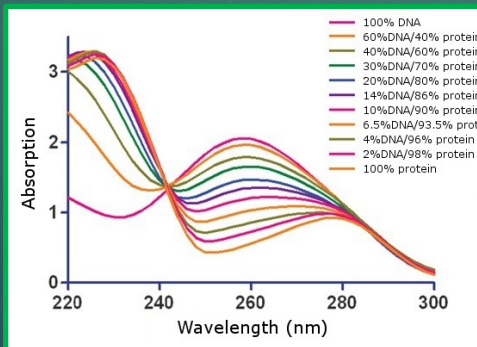
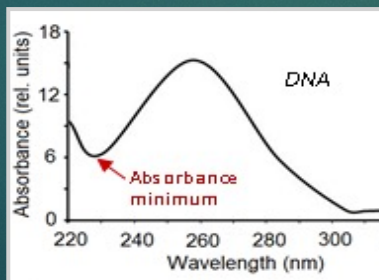
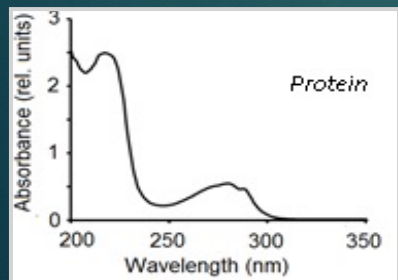
Femtosecond Laser Treatment

Tissue 'optical windows'



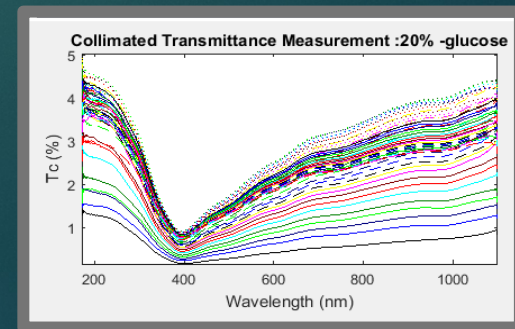
Absorption (μ_a) and reduced scattering (μ'_s) coefficients, and light penetration depth (δ) of peritoneum within tissue 'optical windows'
 Bashkatov A. N. *et al.* *Opt. Spectrosc.* 120 (1), 1-8, 2016; *JBO*, 23 (9) 2018

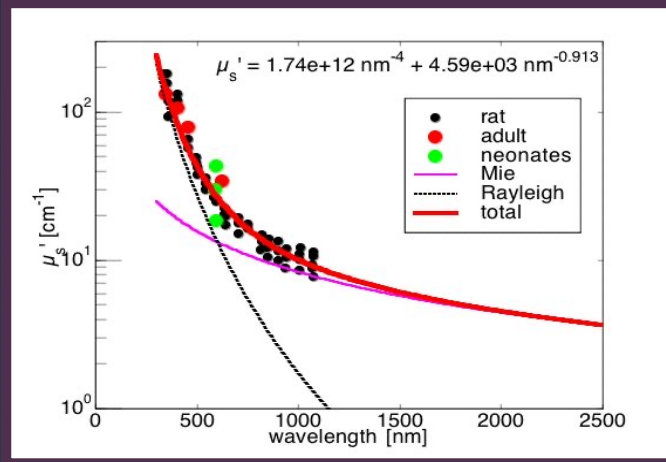
Y. Zhou, et al. *J. Biomed. Opt.* 21(6), 061007 (2016)



Rat muscle treatment with 20% glucose solution

P. Peixoto, et al., *J. Biomed. Photon. Eng* 1(4) 255, 2016

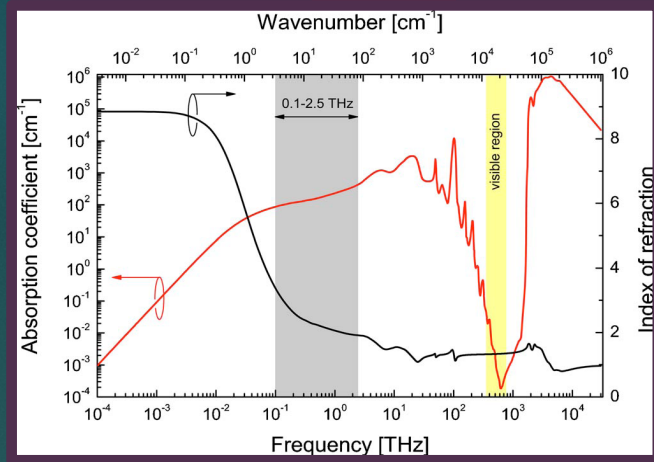




Optical clearing method helps to reduce scattering of tissues

$$\mu_s' = \mu_s(1-g) \sim d^2 \rho (d/\lambda)^{0.37} (m-1)^2$$

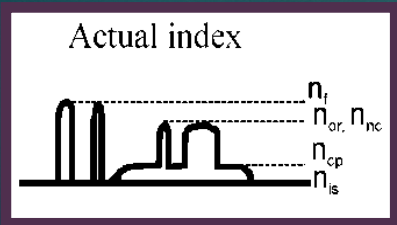
$$m \equiv n_s/n_0$$



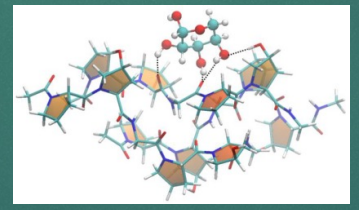
Refractive index matching mechanism

Optical clearing agents

Dehydration mechanism

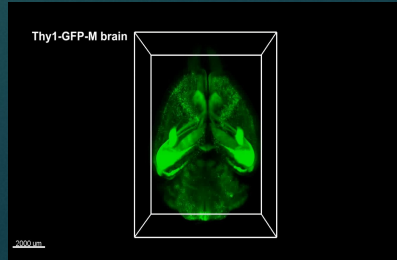
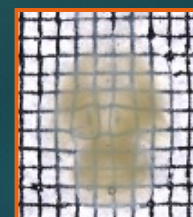
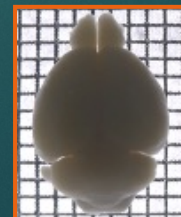
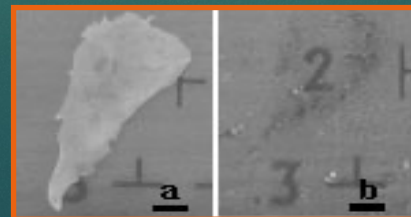
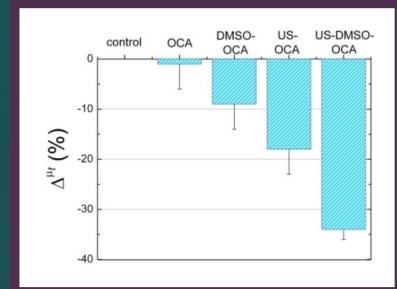


- Hyperosmotic agents:**
- ❖ Glucose
 - ❖ Sorbitol
 - ❖ Glycerol
 - ❖ Polyethylene glycol
 - ❖ Propylene glycol
 - ❖ Dimethyl sulfoxide



- Isosmotic solutions:**
- ❖ X-ray contrast agents: iohexol, iodixanol
 - ❖ MRI contrast agents: gadobutrol, etc.

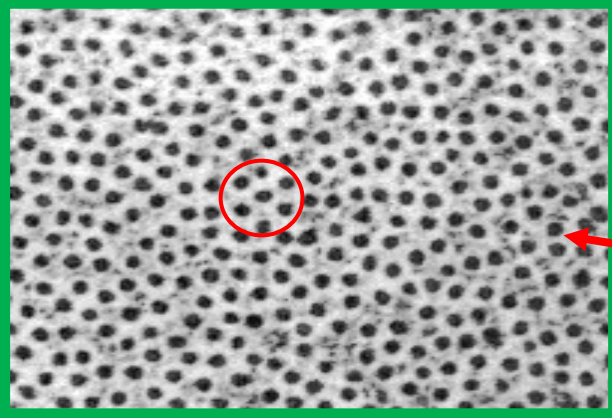
Rat skin *in vivo*



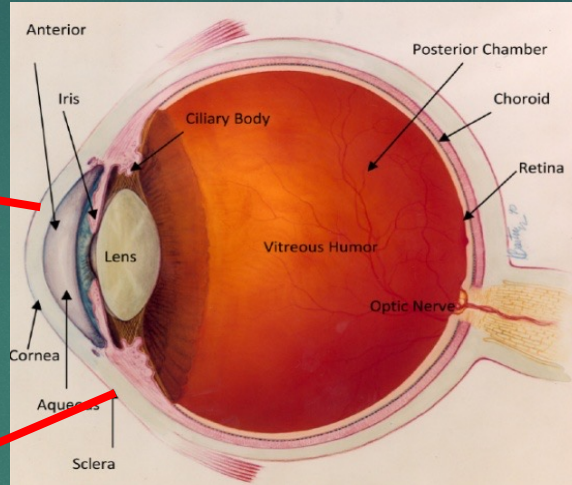
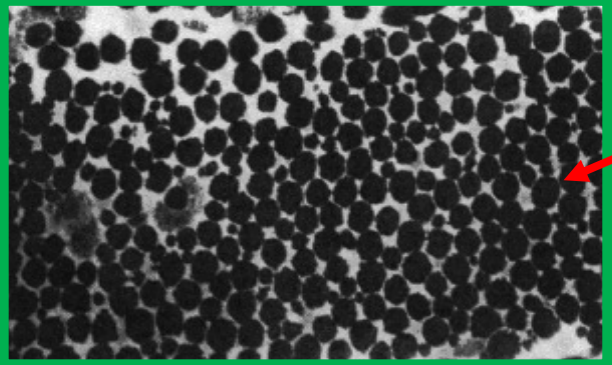
Ordering of collagen fibers



EMI :
Cornea

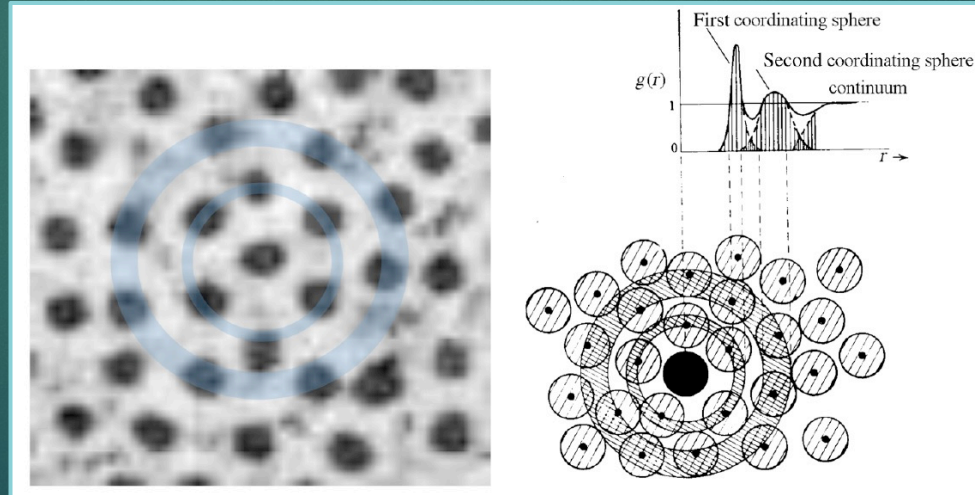
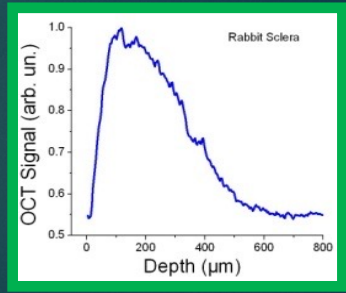
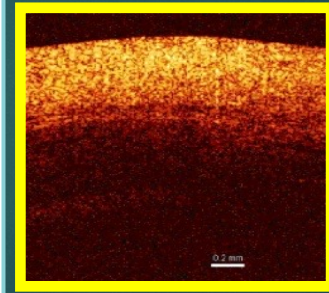
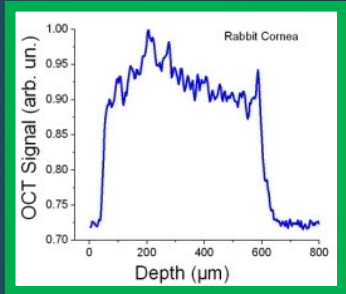
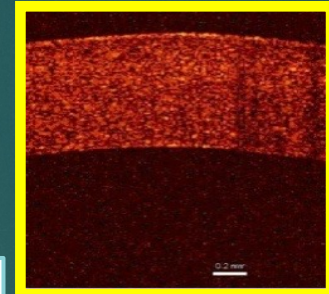


Sclera



OCT : Examples of clear and turbid (scattering) tissues

OCT images and in-depth signal



M.G. Ghosn, V. V Tuchin, K. V. Larin,
IOVS, 2007

V.V. Tuchin, Polarized light interaction with tissues (tutorial), JBO 21(7), 071114 (2016)

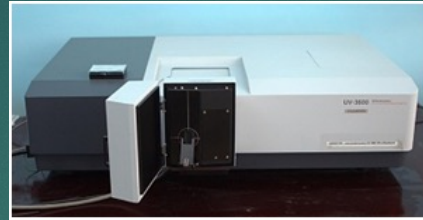
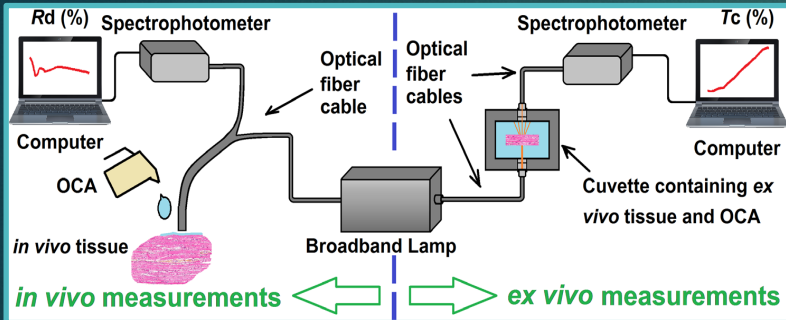
From *Oliveira et al.*, SFM, 2020

Spectral measurements from deep UV to NIR and THz, and OCT of tissues *ex vivo* and *in vivo* + immersion optical clearing (OC)

Spectral measurements *ex vivo/in vivo* + optical clearing



Spectral OCT systems (Thorlabs Inc.)

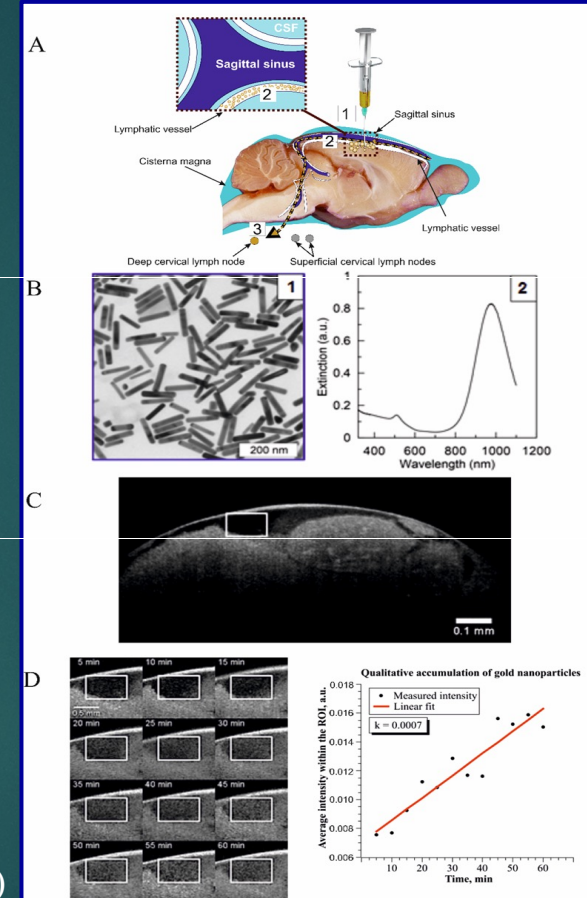


Shimadzu UV-3600, 350-2500 nm
Shimadzu UV-2550, 200-800 nm



OCP930SR 022 (930 nm)

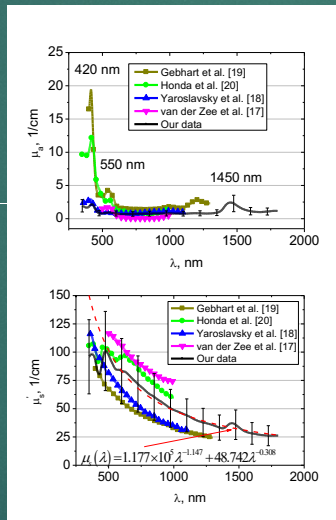
Spectral band, 100 nm
Output power, 2 mW
Scanning depth, 1.6 mm (air)
Axial resolution, 6.2 μm (air)



GANYMEDE, SD-OCT (930 nm)

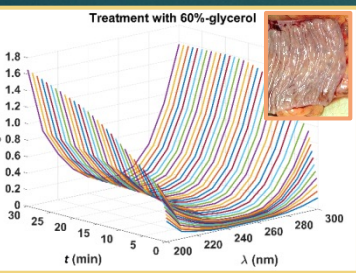
Spectral band, 150 nm
Scanning rate A-scan 29 kHz
Scanning depth, 2.7 mm (air)
Axial resol., 5.8 / 4.4 μm (air/tissue)

Collimated and total transmittance, reflection spectroscopy (fiber-optic and integrating sphere) from deep UV to NIR and THz

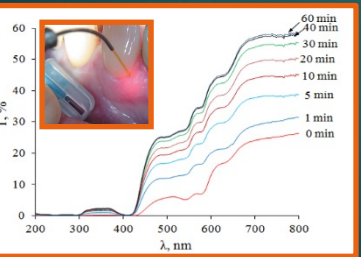
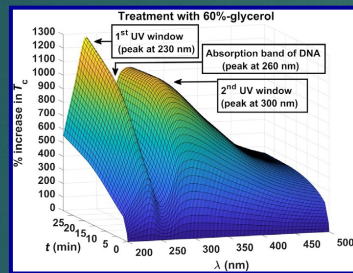


Optical properties of rat brain tissues

The OCT imaging of brain clearing from GNRs: **A** – 1) GNRs are injected into the brain parenchyma; 2) GNRs drain from the brain via the *meningeal lymphatic vessels*; 3) 20 min after injection, GNRs are accumulated in the deep cervical lymph node; **B** – transmission electron microscopy image of GNRs (92×16 nm) (1) and their extinction spectrum (2); **C** – OCT image of the deep cervical lymph node before injection of GNRs; **D** – a set of OCT images illustrating the kinetics of accumulation of GNRs in the deep cervical lymph node; **E** – OCT signal average intensity within the ROI showing linear accumulation of GNRs in the deep cervical node with slope $k = 0.0007$.



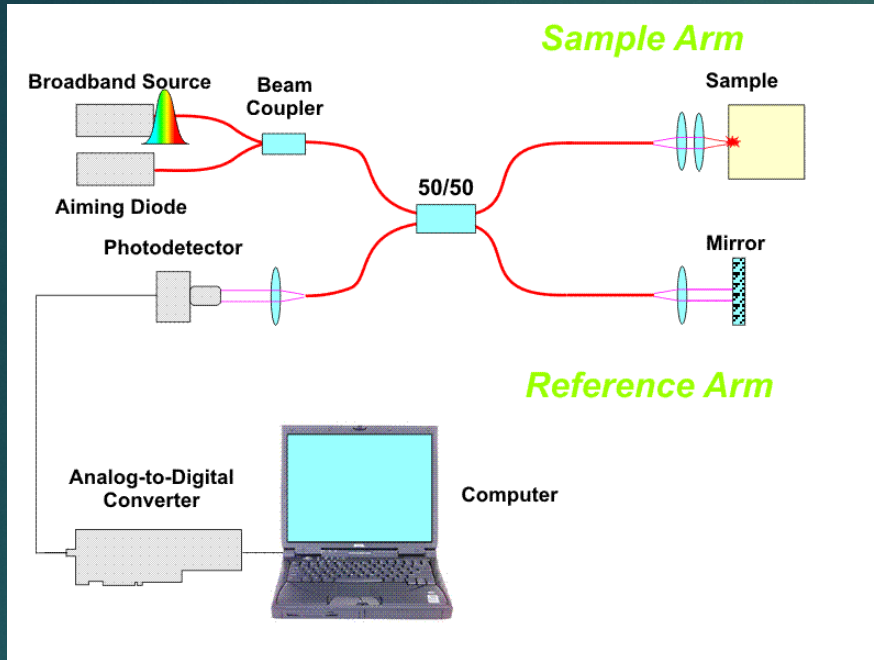
Colorectal muscle, OC efficiency, Glycerol 60%



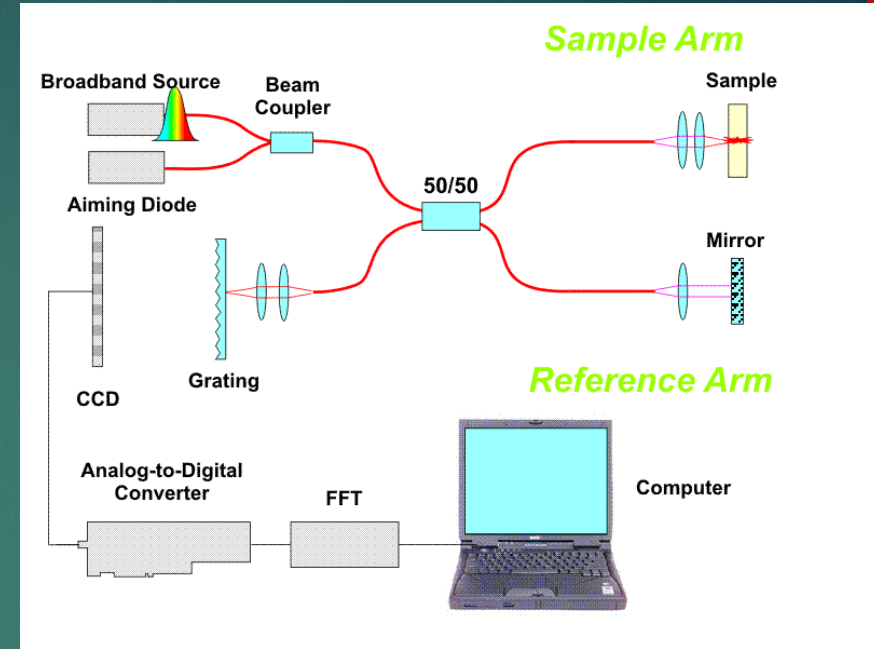
Gingival mucosa, OC efficiency, Glycerol 99.5%

Optical Coherence Tomography

Illustrations are designed by Kirill Larin

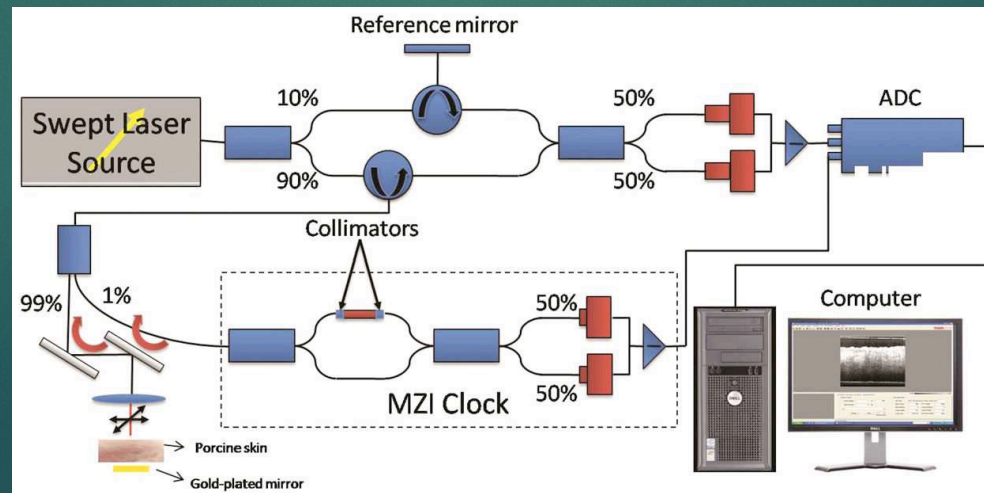


Time domain OCT (TDOCT)



Frequency-domain (spectral) OCT (fOCT)

Swept source OCT (1325 nm)



SS-OCT (Thorlabs, SL1325) setup: MZI: Mach-Zehnder interferometer; ADC: Analog to digital converter

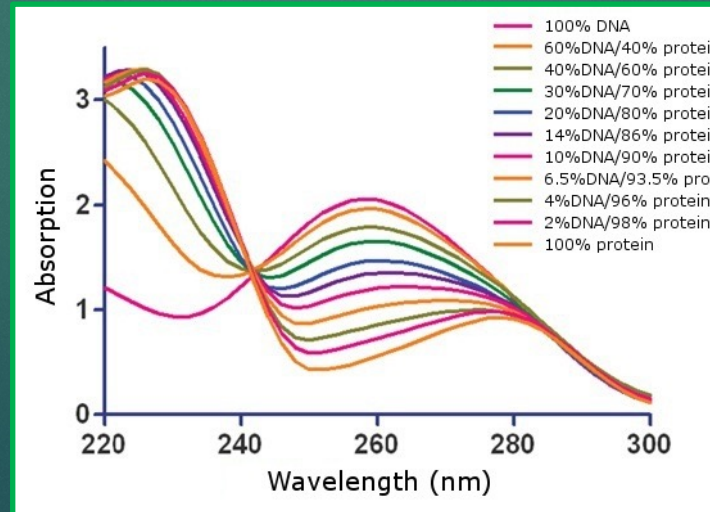
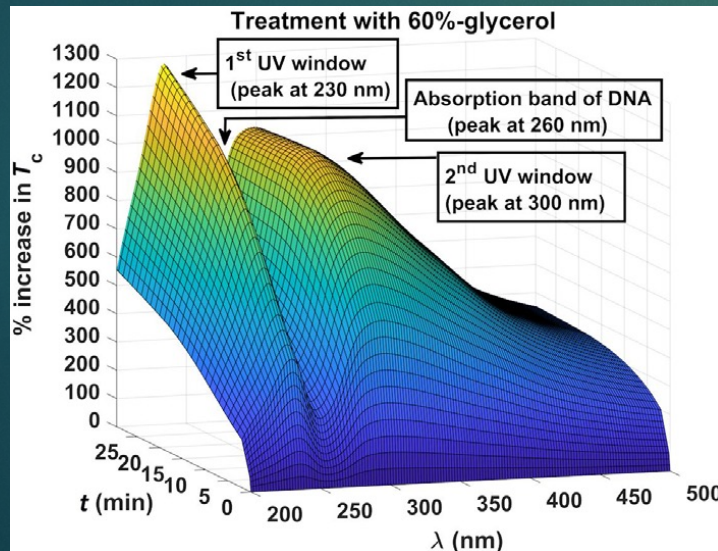
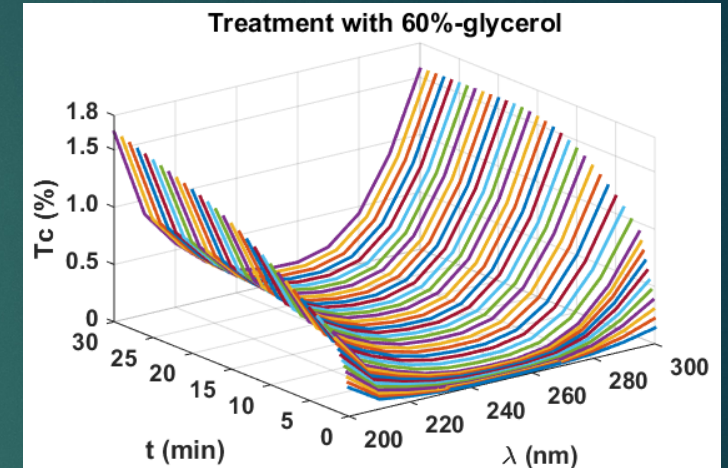
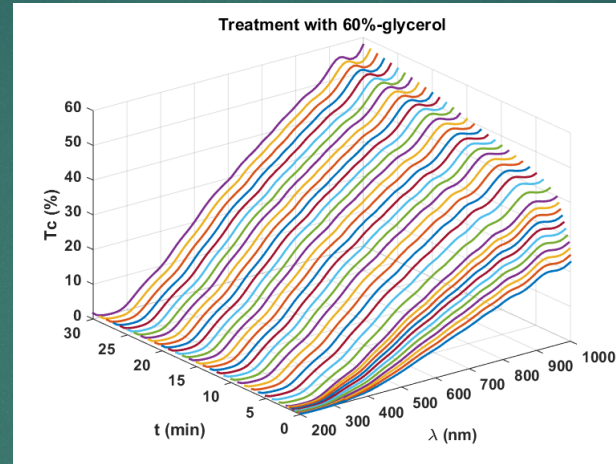
Creation of UV window

I. Carneiro, S. Carvalho, R. Henrique, L. M. Oliveira, V. V. Tuchin, Moving tissue spectral window to the deep-ultraviolet via optical clearing, *J. Biophotonics*. 2019;e201900181.

The sample was immersed in the **glycerol** solution and measurements (200-1000 nm) were acquired during 30 min treatment with a 5 s - time resolution



Surgical colorectal specimen



Similar behavior is observed on both sides of the DNA/Protein absorption band

The OC effect in UV improves with the increase of glycerol concentration in the solution

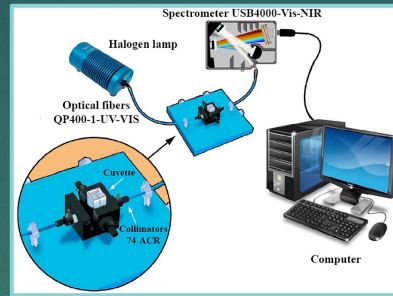
$$\% \text{ increase in } T_c = \frac{T_c(\lambda, t) - T_c(\lambda, t = 0)}{T_c(\lambda, t = 0)} \times 100\%$$

Tissue optical clearing using MRT or CT contrast agents

D.K. Tuchina, I.G. Meerovich, O.A. Sindeeva, V. V. Zherdeva, A. P. Savitsky, A. A. Bogdanov Jr, V. V. Tuchin, Magnetic resonance contrast agents in optical clearing: Prospects for multimodal tissue imaging. *J. Biophotonics* 13(11) 2020; e201960249. <https://doi.org/10.1002/jbio.201960249>

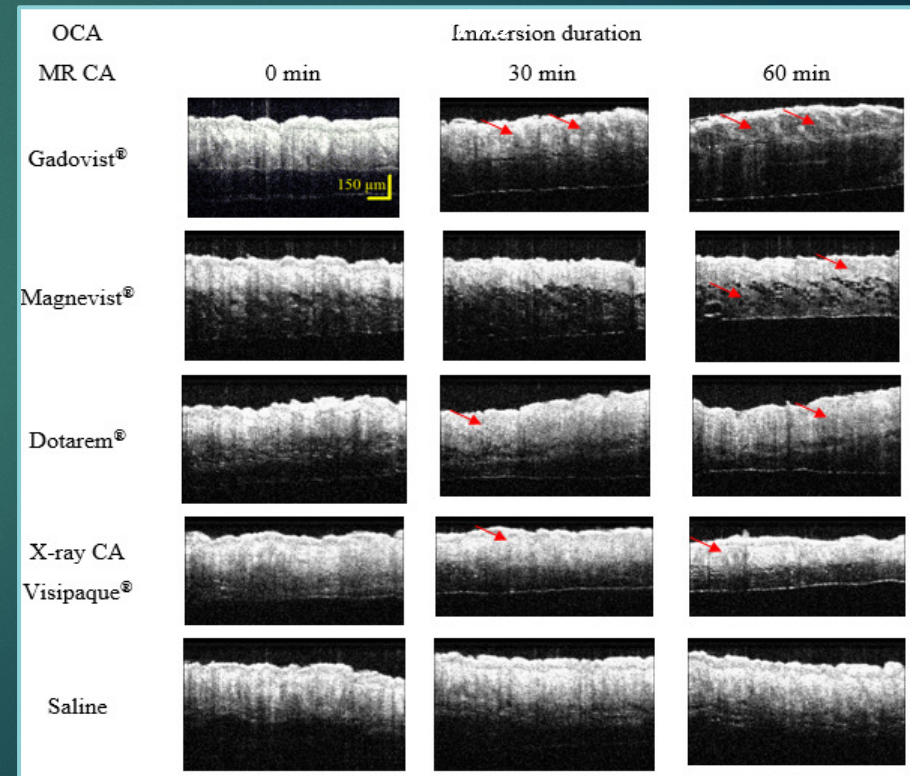
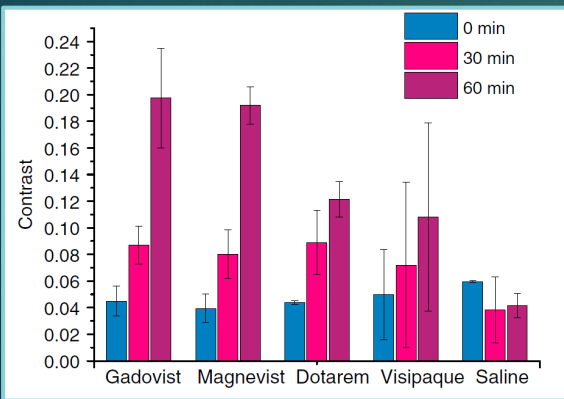
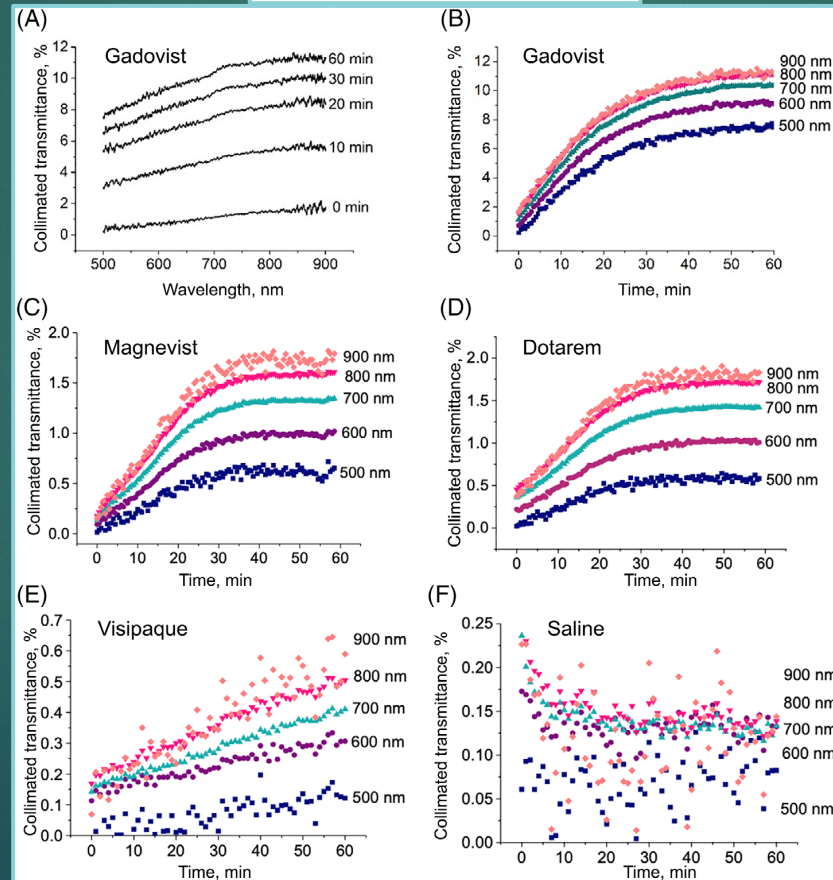
Imaging through albino mouse skin *ex vivo*

MR CA	0 min	30min	60 min
Gadovist®			
Magnevist®			
Dotarem®			
CT CA Visipaque®			
Saline			



❖ **MRI contrasts** can be successfully used as **optical clearing agents** for enhancing optical imaging

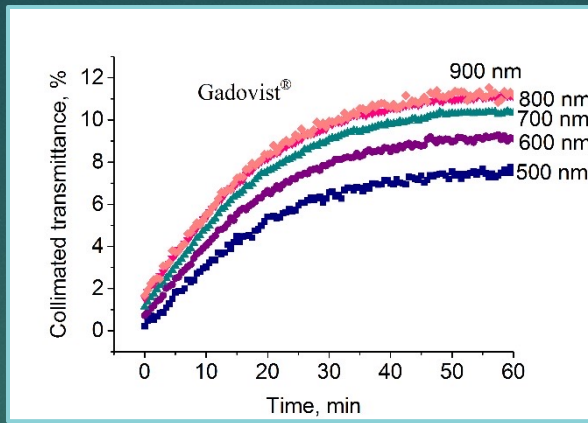
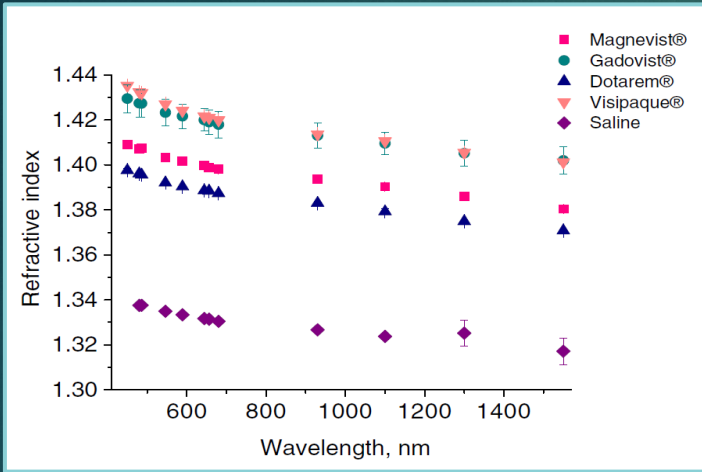
❖ This application clears the path for a fundamentally new approach in multimodal imaging, since synchronization in time and space occurs for enhancement of **optical, CT and MRI** image contrasts
OCT measurements of albino mouse skin *ex vivo*



Administration of MRI agents

Collimated transmittance

Multi-wavelength measurements RI of MRI agents



$$T_c(\lambda) \propto 1 - \exp\left(-\frac{t}{\tau}\right)$$

$$\tau = \frac{L^2}{\pi^2 D_a}$$

$$\frac{l_d}{L} = \sqrt{\frac{D_a^{\text{free}}}{D_a^{\text{tissue}}}}$$

Wavelength, nm	OCE = T_c^{OC} / T_c^0			
	Gadovist	Magnevist	Dotarem	Visipaque
500	32.9 ± 5.5	29.7 ± 4.0	11.3 ± 7.7	7.5 ± 1.2
600	16.0 ± 2.8	16.0 ± 5.7	5.0 ± 1.0	5.0 ± 1.1
700	9.2 ± 0.3	10.5 ± 0.7	3.9 ± 0.1	2.8 ± 0.3
800	7.2 ± 0.2	9.5 ± 0.7	4.4 ± 0.6	2.7 ± 0.2
900	6.5 ± 0.7	9.5 ± 2.1	4.4 ± 0.6	3.8 ± 0.8

MRI agent diffusion coefficients measured in mouse skin *ex vivo*

Agent Trademark	MR				X-ray
	Gadovist	Magnevist	Dotarem	Visipaque	
$D_a^{\text{tissue}}, \text{cm}^2/\text{s}$	$(4.29 \pm 0.39) \times 10^{-7}$	$(5.00 \pm 0.72) \times 10^{-7}$	$(3.72 \pm 0.67) \times 10^{-7}$	$(1.64 \pm 0.18) \times 10^{-7}$	
$D_a^{\text{free}}, \text{cm}^2/\text{s}$	3.9×10^{-6}	—	4.5×10^{-6}	—	
Tortuosity, l_d/L	3.0	—	3.5	—	

□ Gadovist – is the most effective OCA

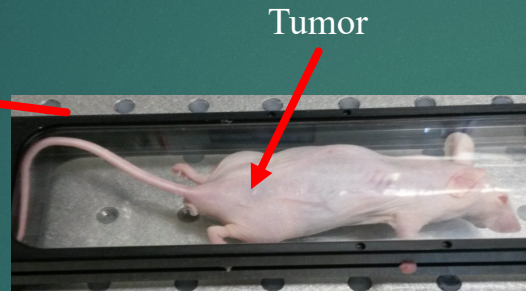
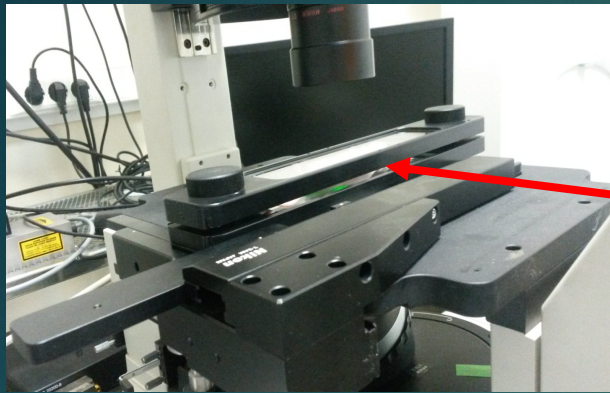
Fluorescence measurements at OC

Fluorescence intensity images of mouse cancer cells *in vivo*

D.K. Tuchina, I.G. Meerovich, O.A. Sindeeva, V. V. Zherdeva, A. P. Savitsky, A. A. Bogdanov Jr, V. V. Tuchin, Magnetic resonance contrast agents in optical clearing: Prospects for multimodal tissue imaging. *J. Biophotonics* 13(11) 2020; e201960249. <https://doi.org/10.1002/jbio.201960249>

20 days after tumor cell enucleation (HEp2-TagRFP line) in BALBc/nude mice

OCA: 70% glycerol, 5% DMSO, 25% water

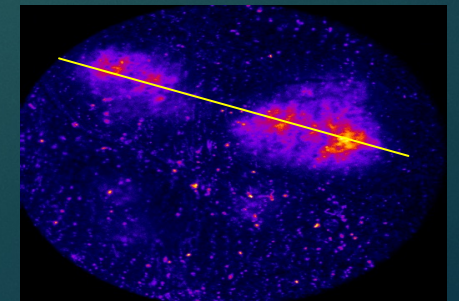
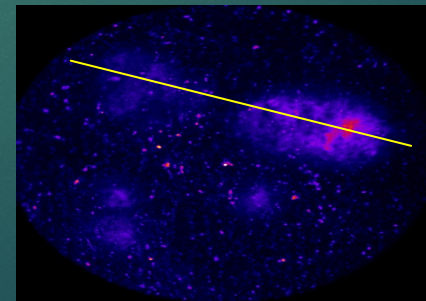
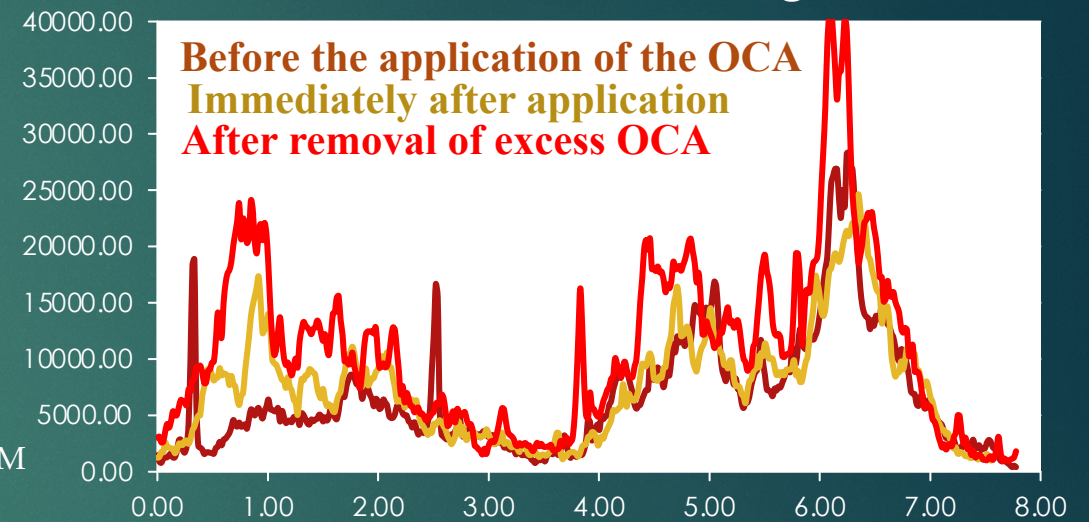


Cassette with animal

Instrumentation and Protocol

- ❖ DCS-120 confocal scanning system (Becker & Hickl GmbH)
- ❖ WhiteLase SC480-10 supercontinuum laser with acousto-optic tunable filter AOTF-V1-D-FDS-SM (FIANIUM)
- ❖ HPM-100-40 hybrid detector (Becker & Hickl GmbH)
- ❖ Fluorescence excitation wavelength was 540 nm
- ❖ Fluorescence emission from a tumor was collected through the skin in the epi-illumination configuration
- ❖ Long- and bandpass filters were used (HQ550LP and 580BP)
- ❖ SPCImage 3.2 data analysis software (Becker & Hickl GmbH).
- ❖ NIH ImageJ 1.48v software
- ❖ Animals were anesthetized by Zoletil-Rometar mixture and were put in a cassette on a mobile stage
- ❖ Optical clearing was performed for 15 min using a **70% glycerol, 5% DMSO, 25% water solution**
- ❖ Image collection time for anesthetized mouse varied from 3.5 to 8 min depending of fluorophore expression level

Profiles for fluorescence signal



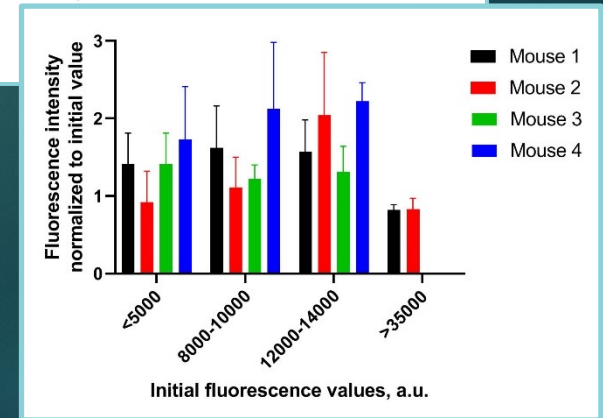
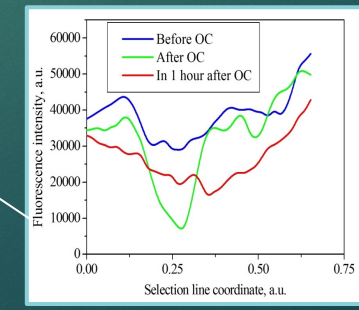
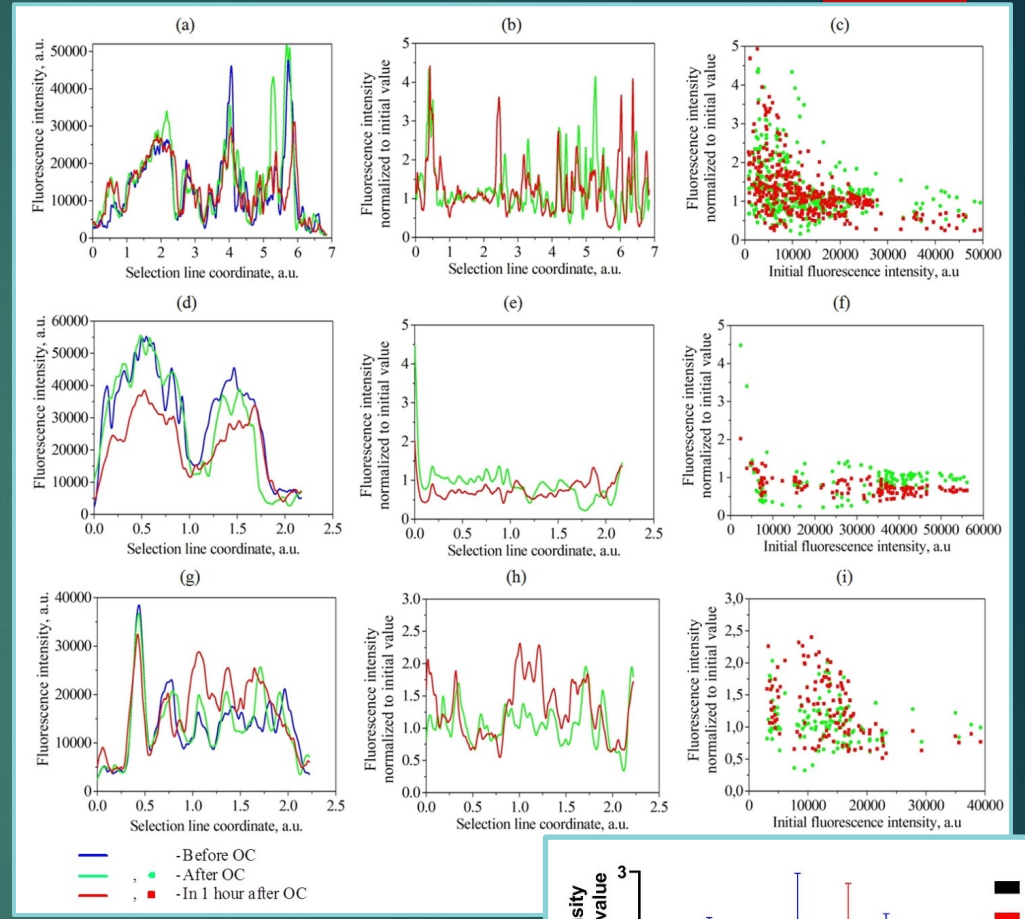
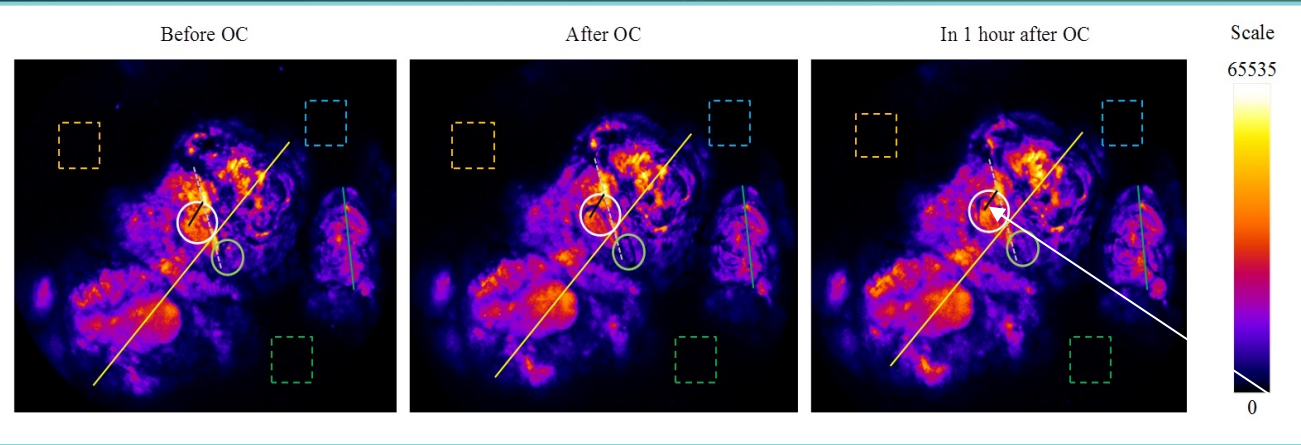
Fluorescence intensity images of mouse cancer cells *in vivo*

D.K. Tuchina, I.G. Meerovich, O.A. Sindeeva, V. V. Zherdeva, A. P. Savitsky, A. A. Bogdanov Jr, V. V. Tuchin, Magnetic resonance contrast agents in optical clearing: Prospects for multimodal tissue imaging. *J. Biophotonics* 13(11) 2020; e201960249. <https://doi.org/10.1002/jbio.201960249>

20 days after tumor cell enucleation (HEp2-TagRFP line) in BALBc / nude mice

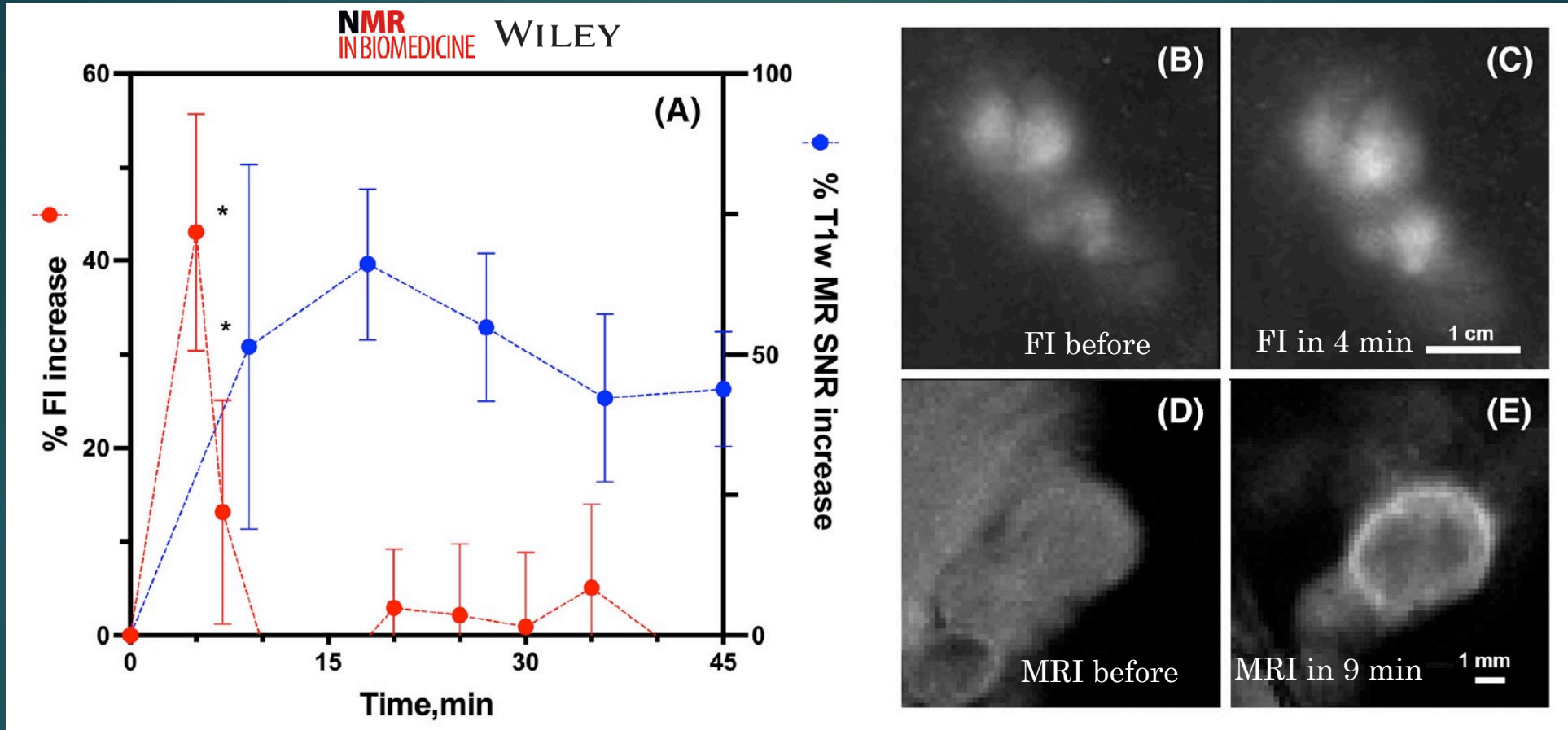
OCA: Gadobutrol (GB) Gadovist®

Protocol	Time, min																						
	1-10	11-15	16-17	18	19	20-34	35	36-37	38-39	40	41-66	67	68-69	70	71-96	97	98-99	100	101-111	112	113-114	115	
	Before OC			OC	After OC			In 30 min			In 60 min			In 75 min									
Anesthesia and placing the animal in a cassette	█																						
Measurement setup	█	█																					
Measurements			█	█																			
Data storage																							
Cassette opening																							
OCA application							█	█															
Cassette closing																							
Measurement setup																							
Measurements																							
Data storage																							



Tag-RFP fluorescence and MRI of tumor mouse xenografts after an intravenous injection of GB

N.I. Kazachkina, V.V. Zherdeva, I.G. Meerovich, A.N. Saydasheva, I.D. Solovyev, D.K. Tuchina, A.P. Savitsky, V.V. Tuchin, A.A. Bogdanov Jr., "MR and fluorescence imaging of gadobutrol-induced optical clearing of red fluorescent protein signal in an in vivo cancer model," *NMR in Biomedicine*, e4708-1-13 (2022).



A: Time course of FI and T1w MRI SNR measured using whole tumor ROIs after an intravenous injection of GB (0.3 mmol/kg, $n = 3$). Data shown as mean \pm SD. Asterisks indicate that measured means are statistically significant from the baseline values ($P < 0.01$).

B: Tag-RFP FI imaging before intravenous injection of GB.

C: Tag-RFP FI imaging 4 min after intravenous injection of GB

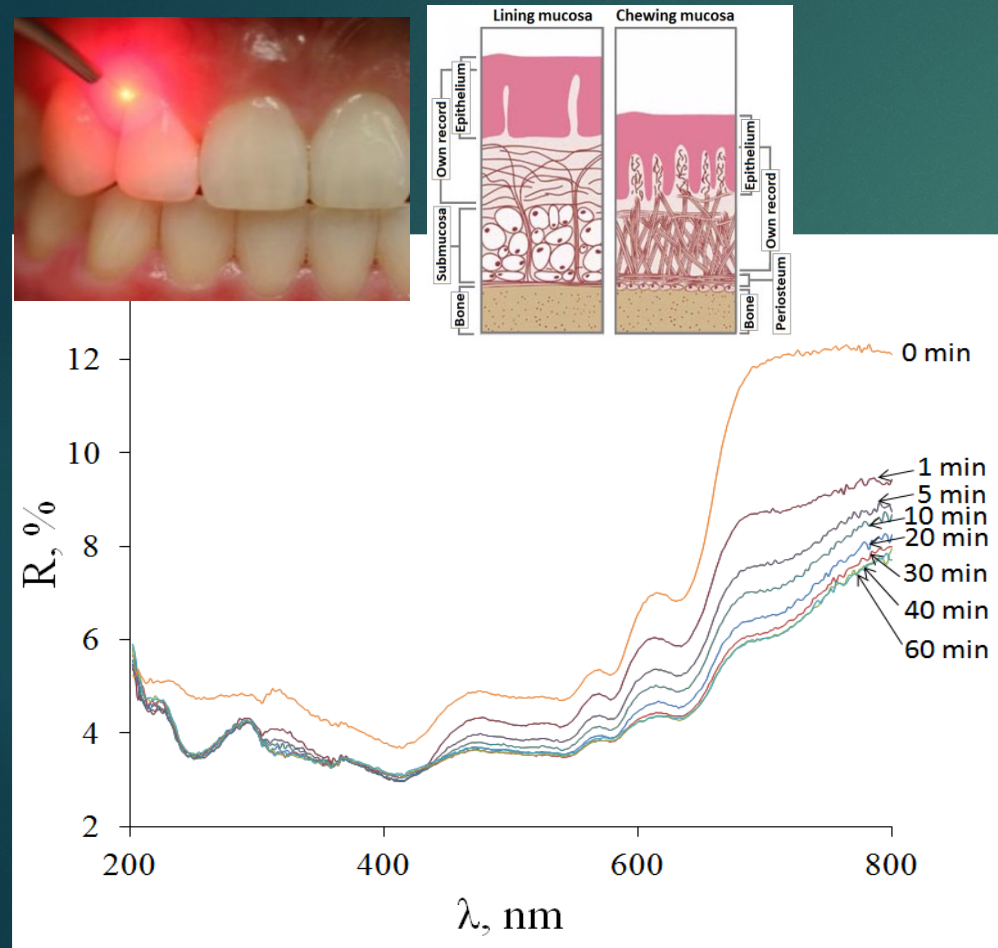
D: Single sagittal MR slice, T1w GRE MRI of the tumor before intravenous injection of GB.

E: Matching single sagittal slice, T1w GRE MRI of the tumor 9 min after intravenous injection of GB; bar, 1 mm

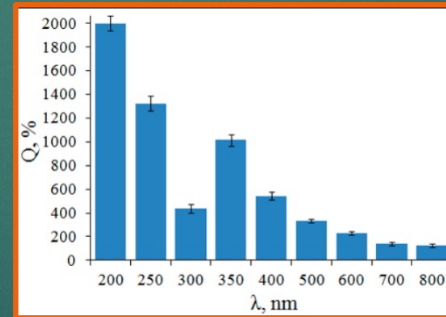
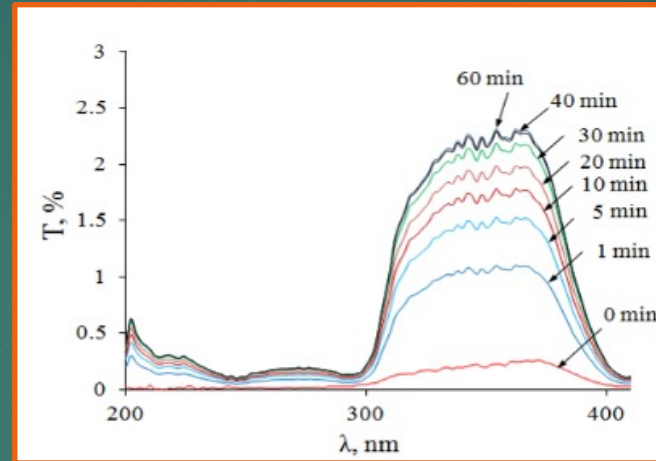
The effectiveness of human gingival tissue OC and therapy

A.A. Selifonov and V.V. Tuchin, Control of the optical properties of gums and dentin tissue of a human tooth at laser spectral lines in the range of 200 – 800 nm, *Quantum Electronics*, 50 (1), 47-54 (2020)

I. Carneiro, S. Carvalho, R. Henrique, A. Selifonov, L. Oliveira, V.V. Tuchin, Enhanced ultraviolet spectroscopy by optical clearing for biomedical applications, *IEEE Journal of Selected Topics in Quantum Electronics* 27 (4), 7200108-1-8 (2021)

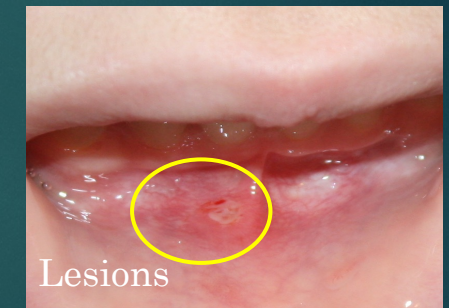


OCA: 99.7% glycerol



A.A. Selifonov – PhD thesis on study of biophysics of control optical properties of biological tissue to optimize phototherapy for oral cavity diseases

The UV treatment of 120 patients with chronic stomatitis in children's clinic No. 3 in Saratov showed high efficiency for 4-6 procedures



The effectiveness of human gum OC in propylene glycol / glycerol / water mixture
E-cigarette vapor liquid



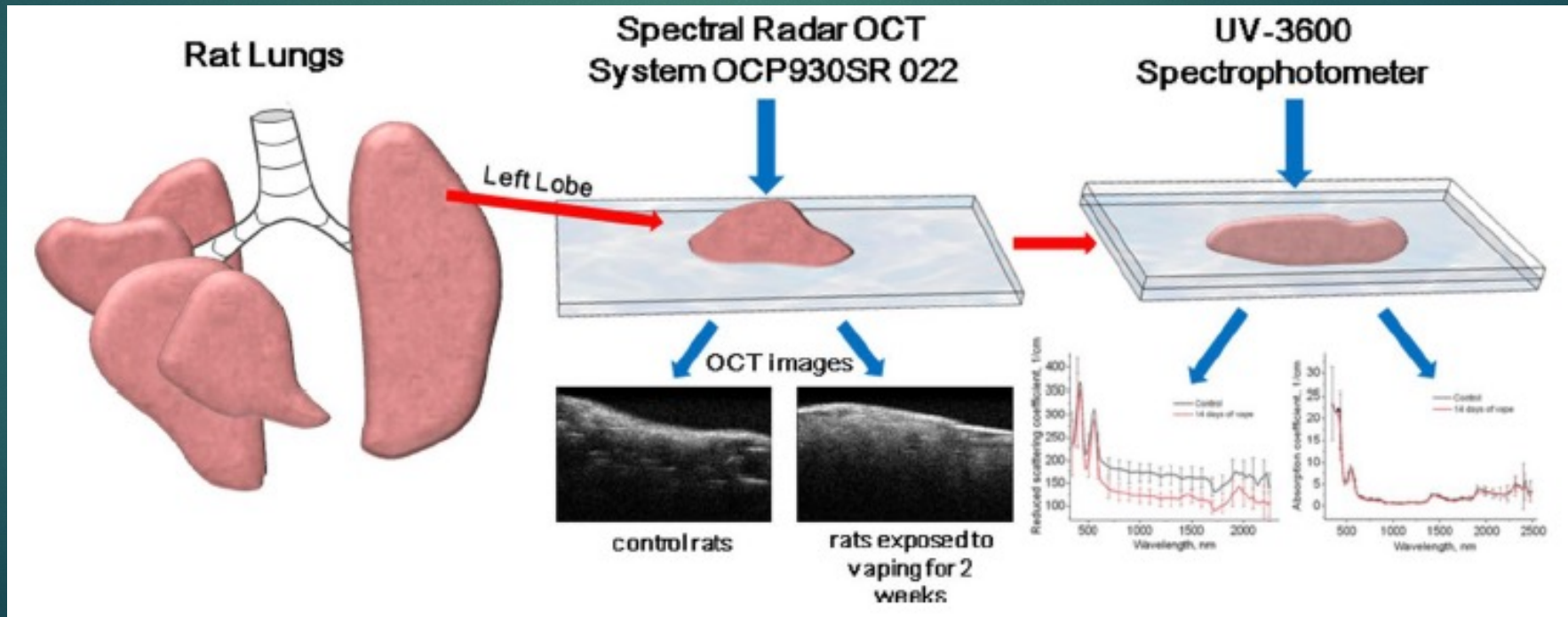
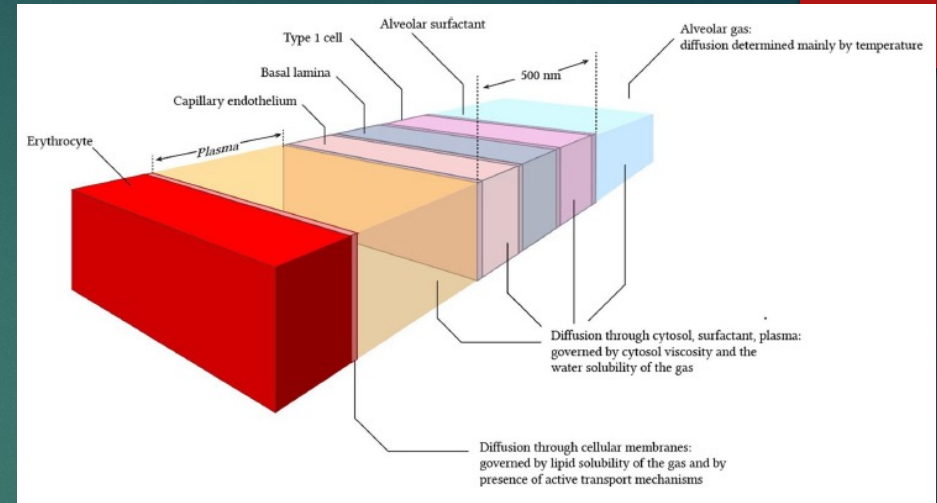
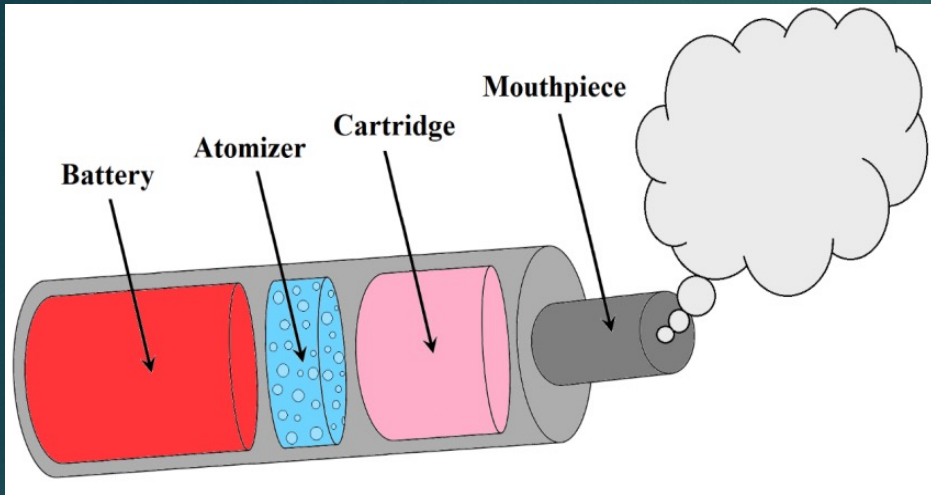
The effective diffusion coefficient in human gum mucous tissue measured *in vitro*:

$$D(30/70/0) = (2.3 \pm 0.4) \cdot 10^{-6} \text{ cm}^2/\text{s}$$

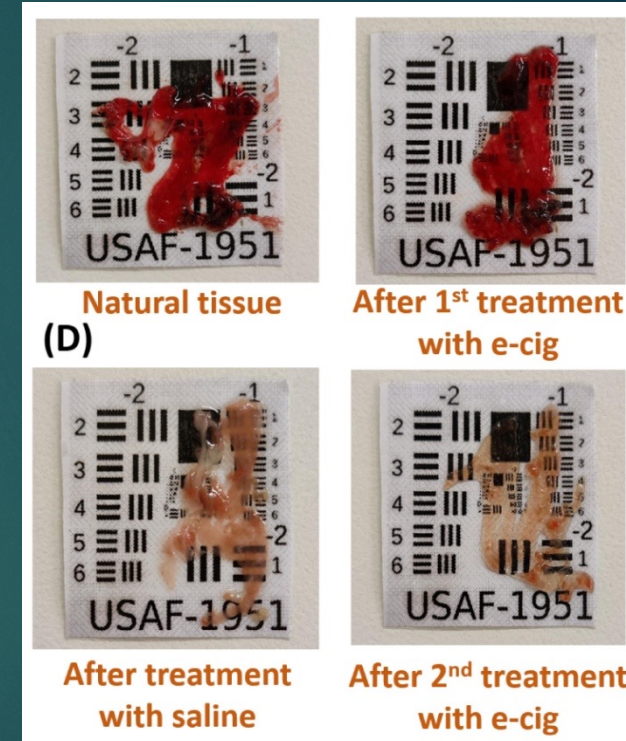
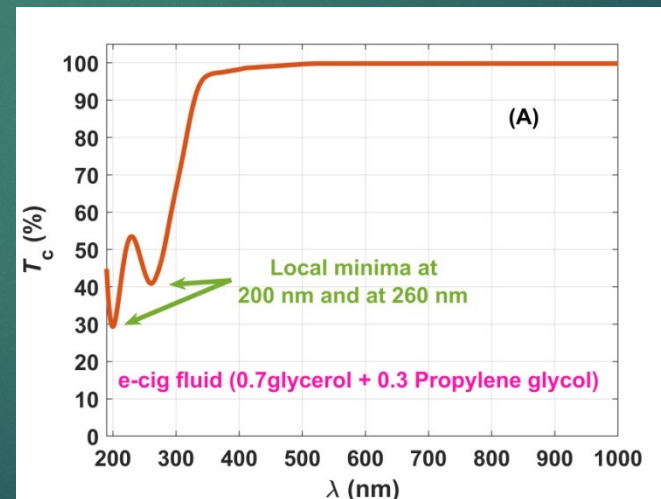
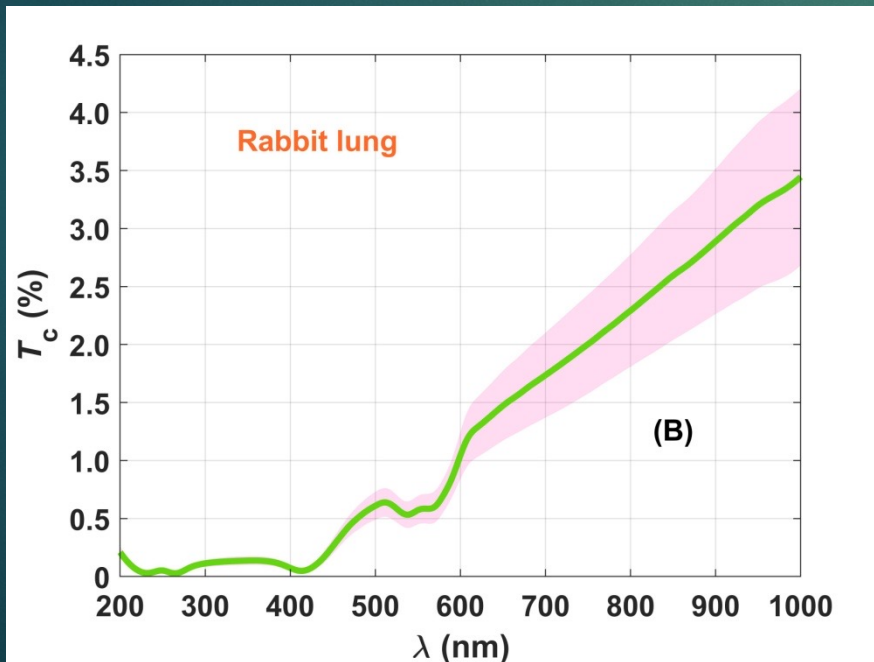
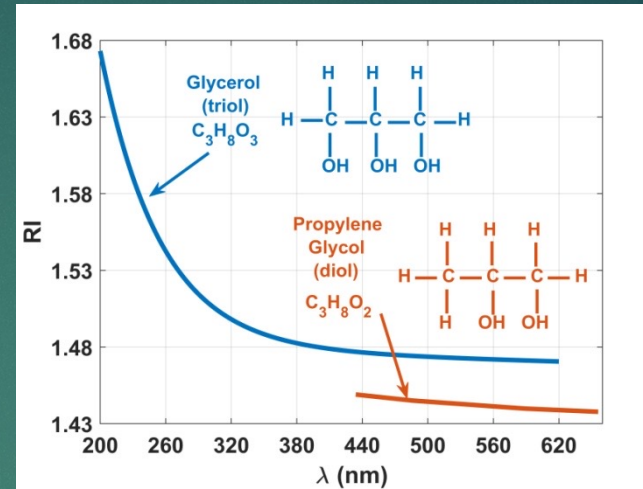
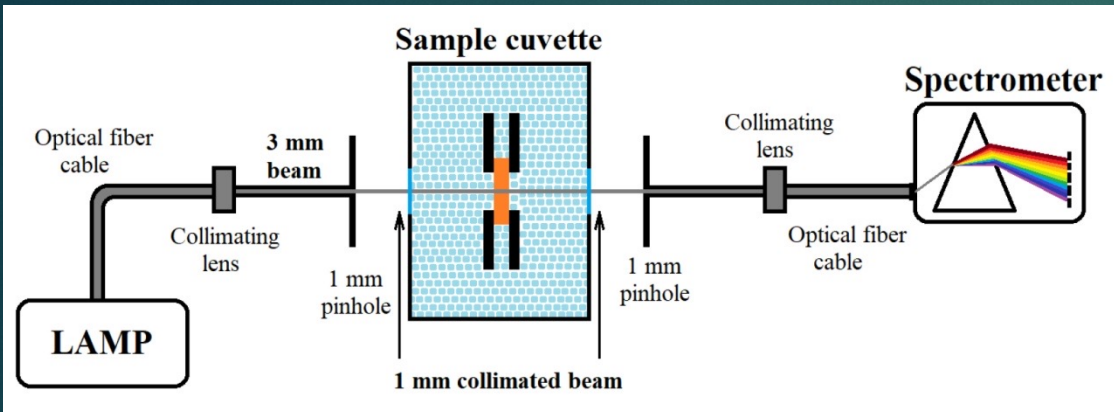
$$D(50/50/0) = (2.6 \pm 0.6) \cdot 10^{-6} \text{ cm}^2/\text{s}$$

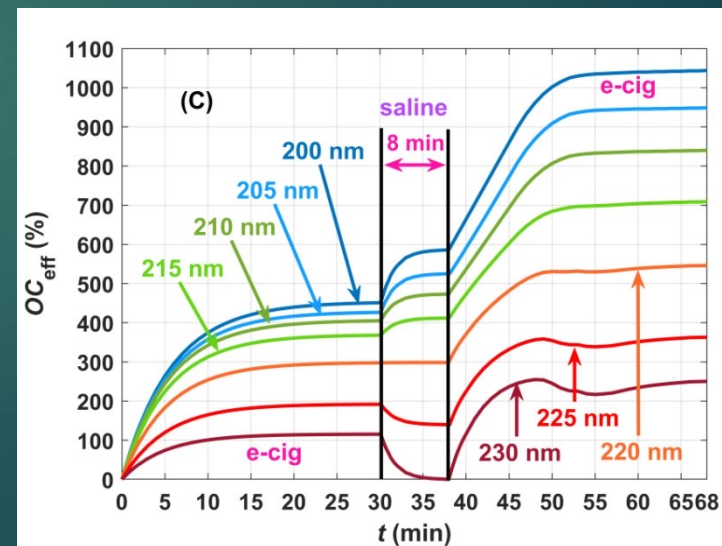
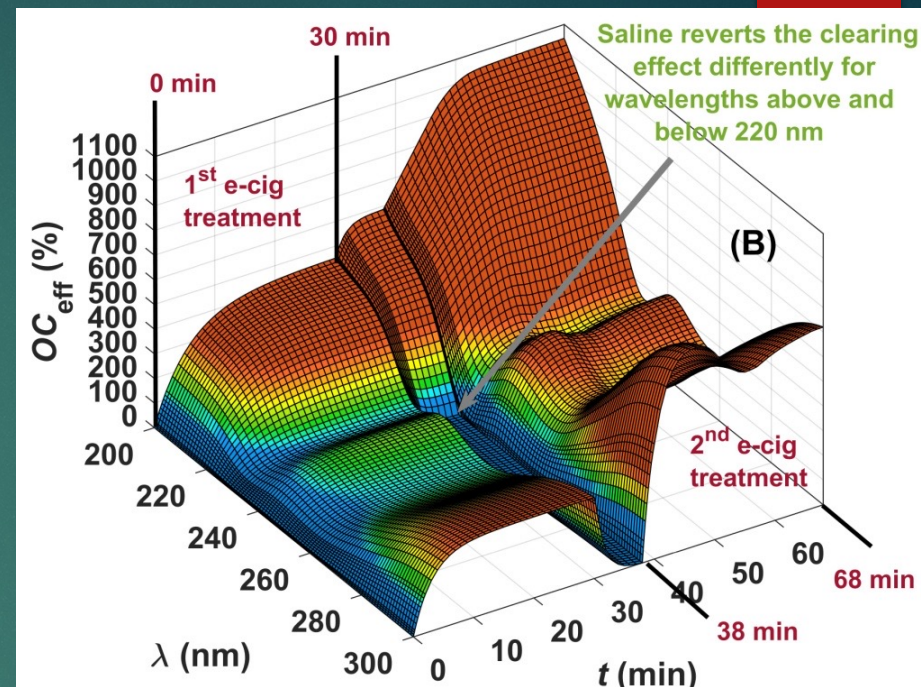
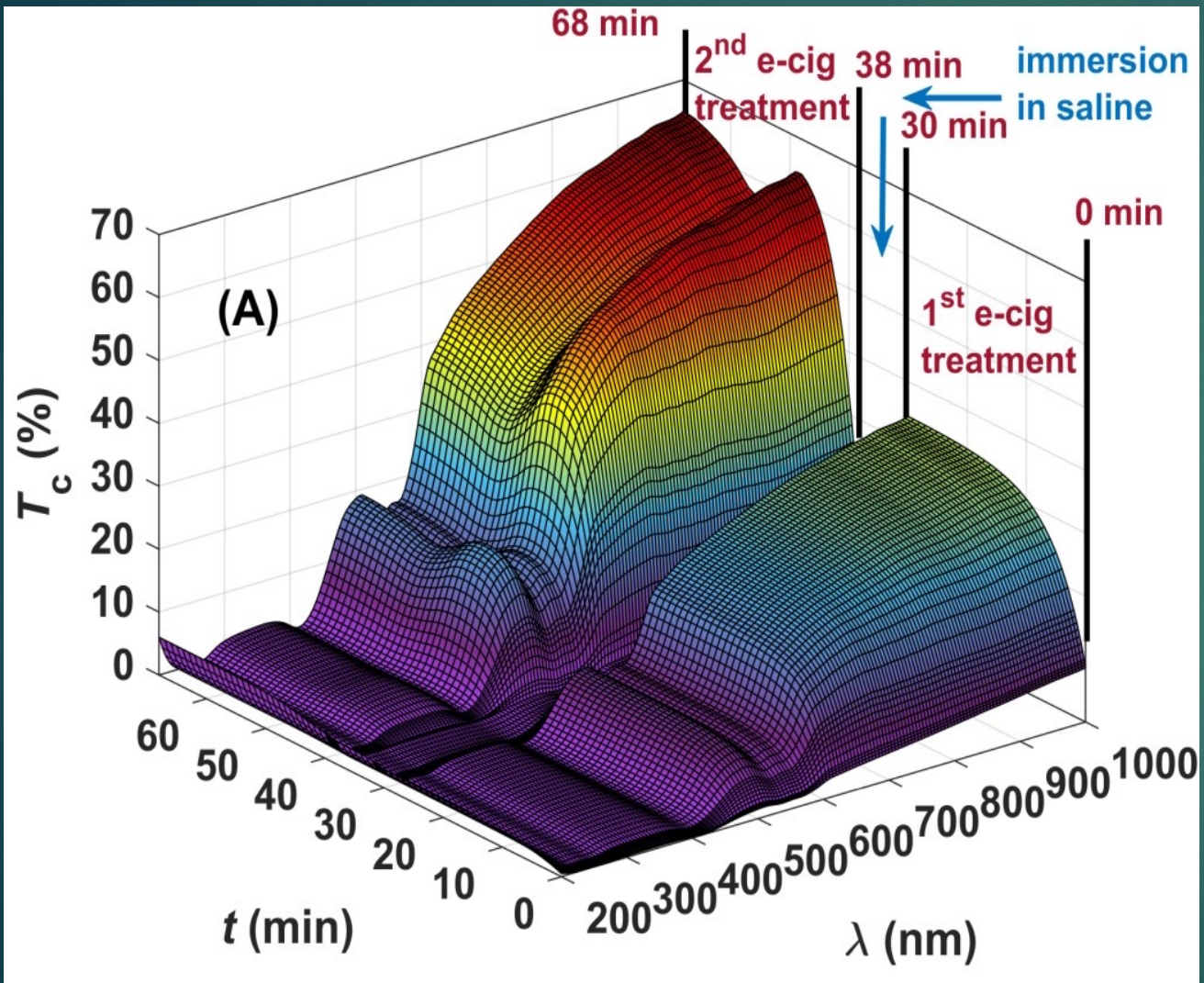
$$D(55/35/10) = (3.2 \pm 0.8) \cdot 10^{-6} \text{ cm}^2/\text{s}$$

A.B. Bucharskaya, et al., Optical clearing and testing of lung tissue using inhalation aerosols: prospects for monitoring the action of viral infections, *Biophysical Reviews* (2022).



L.R. Oliveira, R.M. Ferreira, M.R. Pinheiro, H.F. Silva, V.V. Tuchin, L.M. Oliveira, Broadband spectral verification of optical clearing reversibility in lung tissue, *J. Biophotonics* (August. 2022)

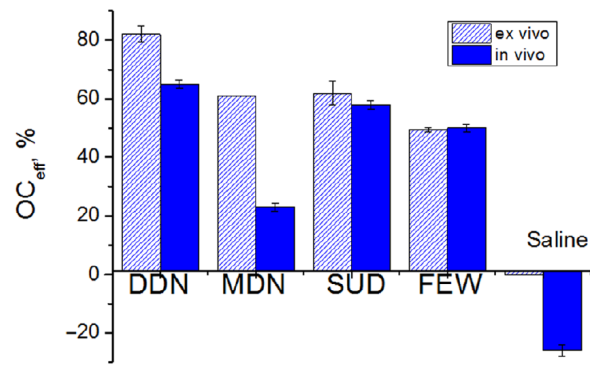
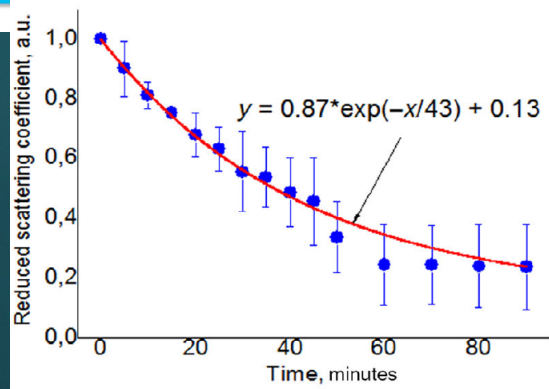
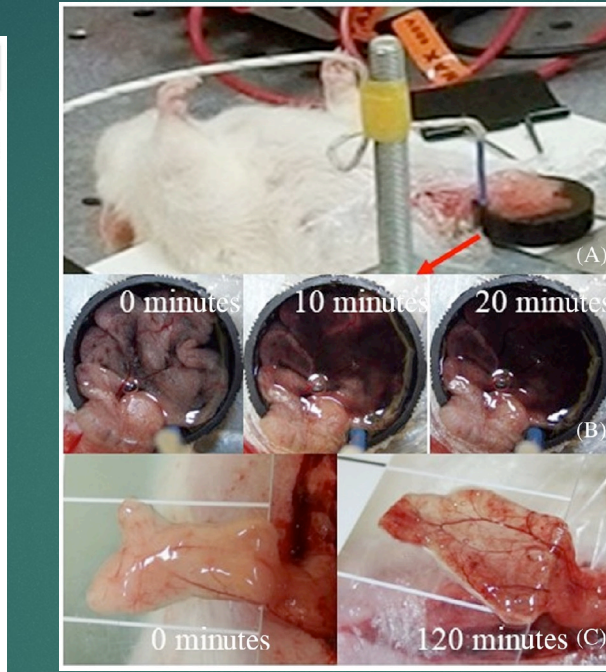
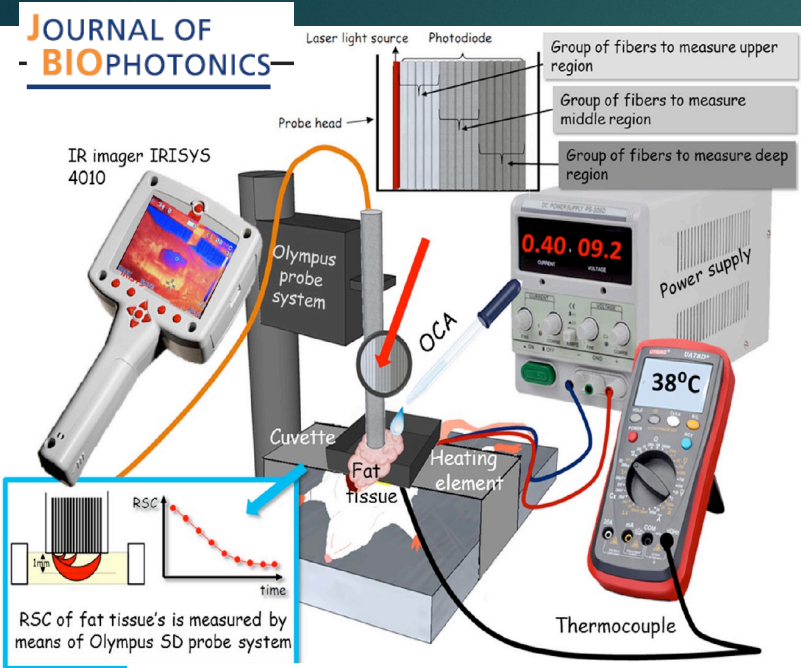




In vivo immersion optical clearing of adipose tissue

Motivation: Conventional or Laser Surgery, to see and avoid dissection of blood vessels

I. Y. Yanina, et al., "Immersion optical clearing of adipose tissue in rats: ex vivo and in vivo studies," *J. Biophotonics* e202100393 (2022)



Ex vivo	Intact	FEW	DDN	MDN	SUD
Damage severity		Low	Middle	Middle	Above middle
Signs		Cells have round shape with thickened membranes	Nuclei are absent, membranes are crenulated	Nuclei are absent, membranes are thickened, eosinophilic and thinned	Broken adipocyte septa
Histological images					
In vivo	Intact	FEW	DDN	MDN	SUD
Damage severity		Low	Middle	Middle	Middle
Signs		Single broken or crenulated adipocyte septa	Swelling of the intercellular membranes of adipose tissue	Severe vascular hyperemia and moderate thickening of membranes	The diapedesis hemorrhages
Histological images					



1 FEW: 50% Fructose, 30% Ethanol, 20% Water (n=1.408)

2 DDN: 21% Diatrizoic acid, 66% DMSO, 13% N-methyl-glucamine (n=1.511)

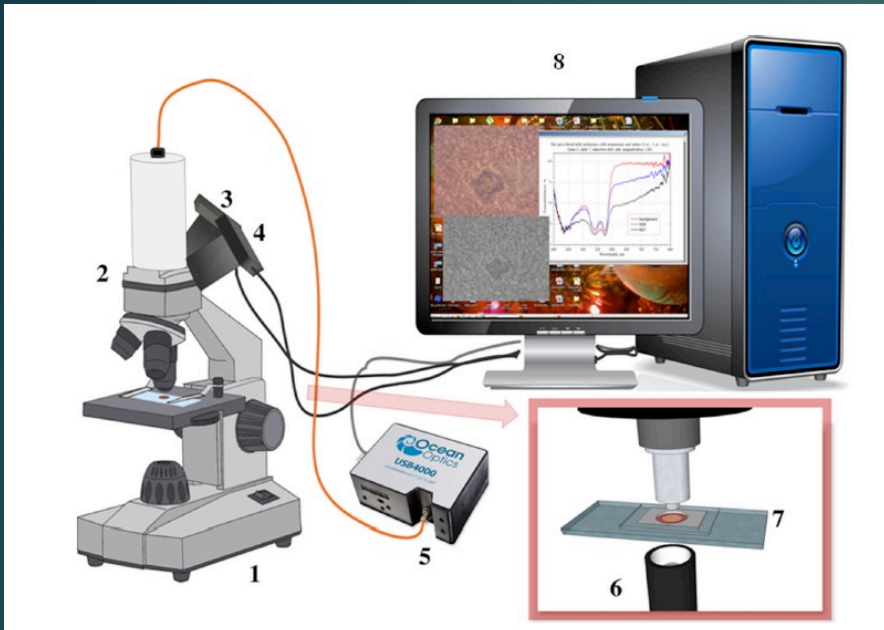
3 MDN: 30% Metrizoic acid, 58% DMSO, N-methyl-glucamine (n=1.529)

4 SUD: 60% Sucrose, 40% DMSO (n=1.509)

Detection of Melanoma Cells in Whole Blood Samples Using Spectral Imaging and Optical Clearing

Polina A. Dyachenko , Leonid E. Dolotov, Ekaterina N. Lazareva, Anastasia A. Kozlova, Olga A. Inozemtseva, Roman A. Verkhovskii, Galina A. Afanaseva, Natalia A. Shushunova, Valery V. Tuchin , Ekaterina I. Galanzha, and Vladimir P. Zharov

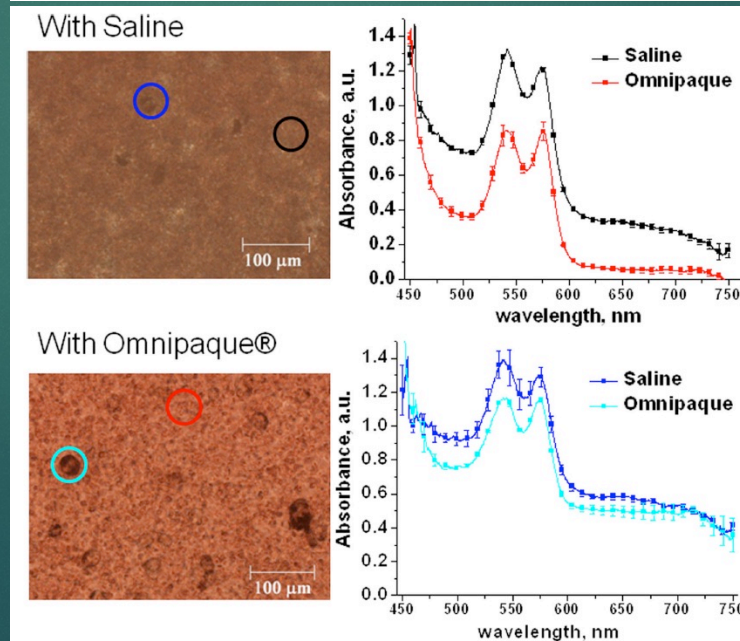
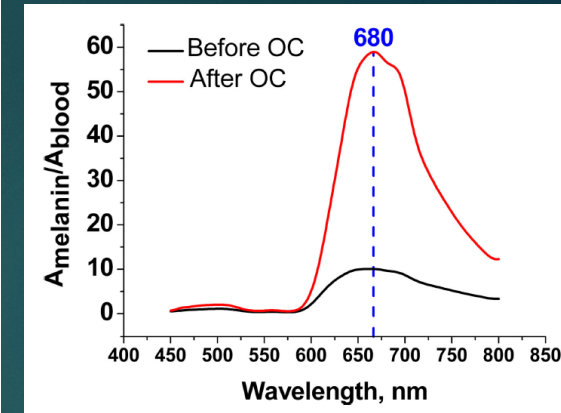
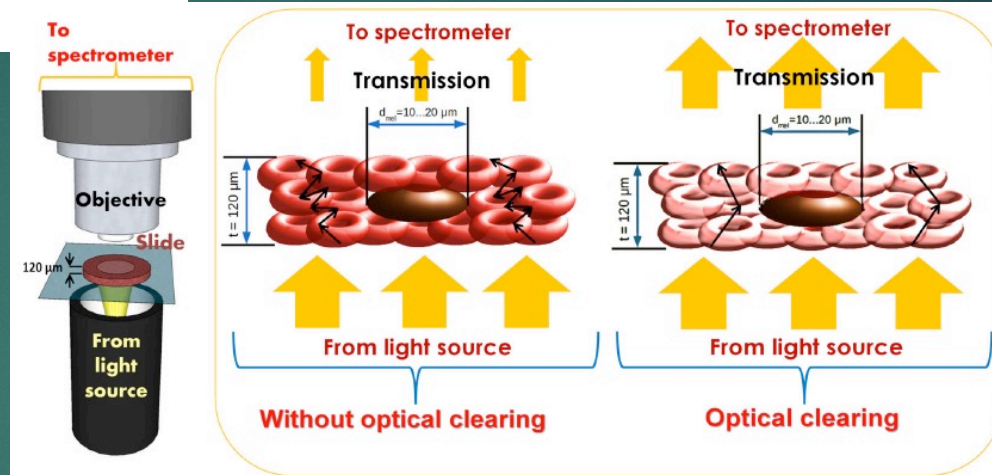
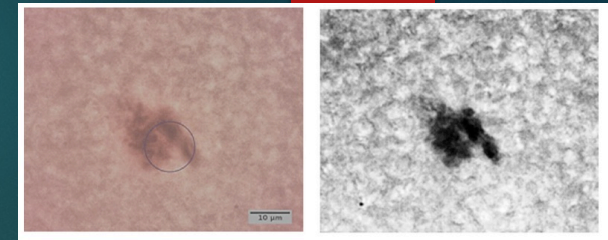
(Invited Paper)



Scheme of experimental setup for spectral study: 3 is the color video camera DCC1645C, 4 is the monochrome camera DCC1545M, 5 is the spectrometer USB4000, 6 is the illumination unit KL-1500Z, 7 is the blood slide



Principle of spectral absorbance measurement of a whole blood sample at immersion OC

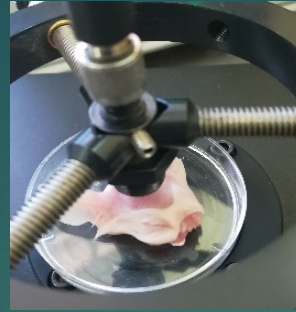


Images of slides of thickness $120 \mu\text{m}$ with a whole blood ($3 \mu\text{l}$) of a laboratory mouse and mouse melanoma cells (B16F10) ($1 \mu\text{l}$) mixed with $4 \mu\text{l}$ of saline (upper image) or Omnipaque (lower image)

Mouse scalp optical clearing by 70%-Glycerol solution + 5% DMSO

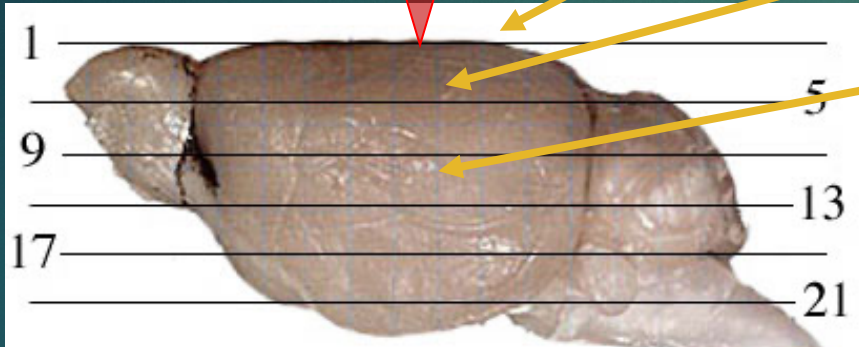


Laser beam
1268 nm

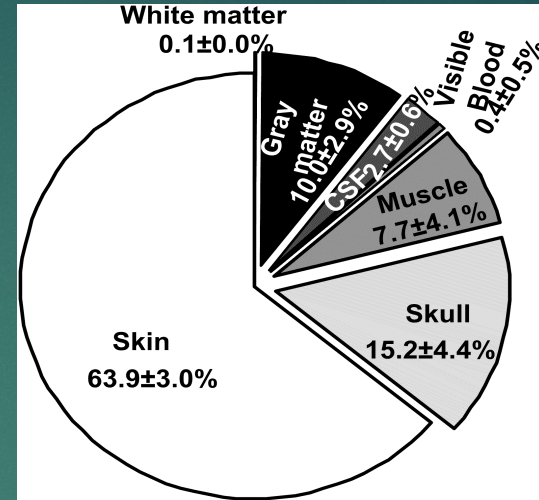


Scalp
Skull

Dura mater Cortex
CSF Gray matter

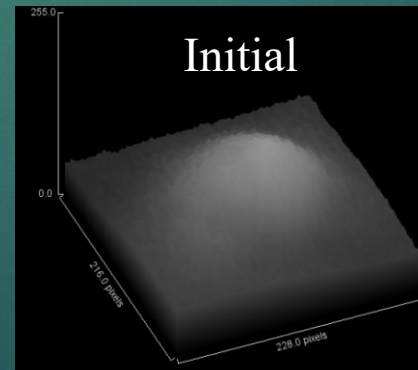
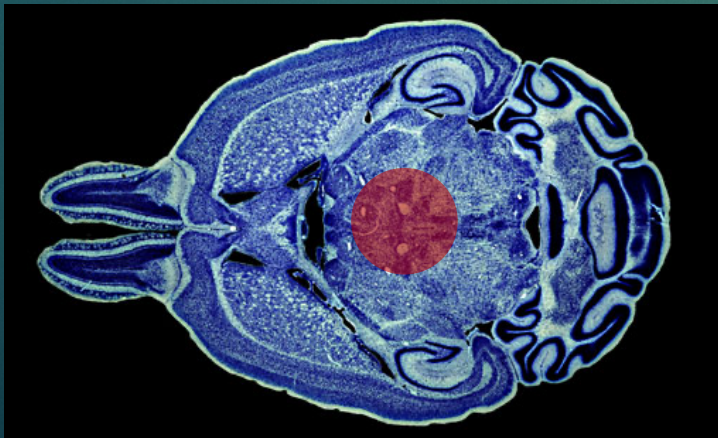
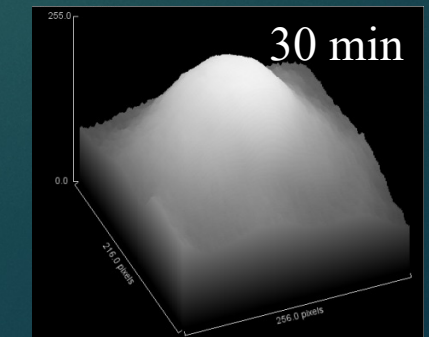
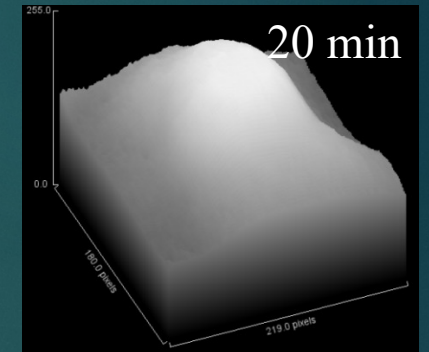
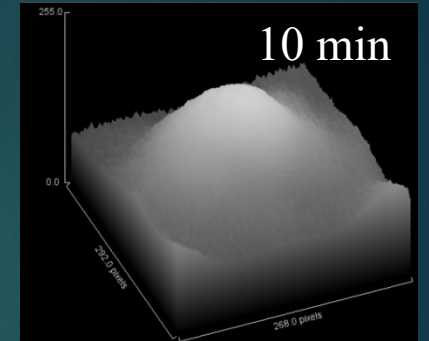


White matter



T. Li, et al. J. Innov. Opt. Health Sci.10(5), 1743002 (2017).

For mouse brain laser beam cross section in the plane 13, total thickness is 7 mm



Increasing the penetration depth for ultrafast laser tissue ablation using Glycerol based optical clearing

Ilan Gabay^a, Kaushik G. Subramanian^a, Chris Martin^a, Murat Yildirim^a, Valery V. Tuchin^{c,d,e}, and Adela Ben-Yakar^{a,b}

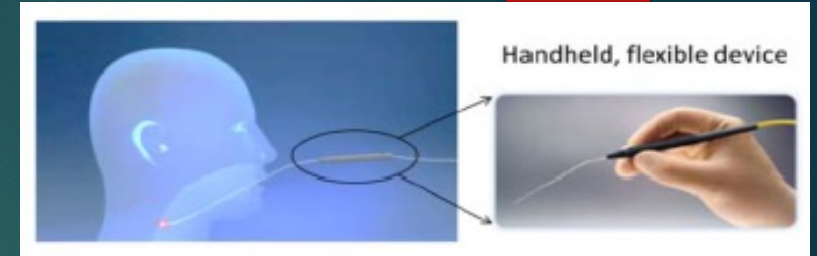
^a Department of Mechanical Engineering, The University of Texas at Austin, Austin, TX, USA

^b Department of Biomedical Engineering, The University of Texas at Austin, Austin, TX, USA

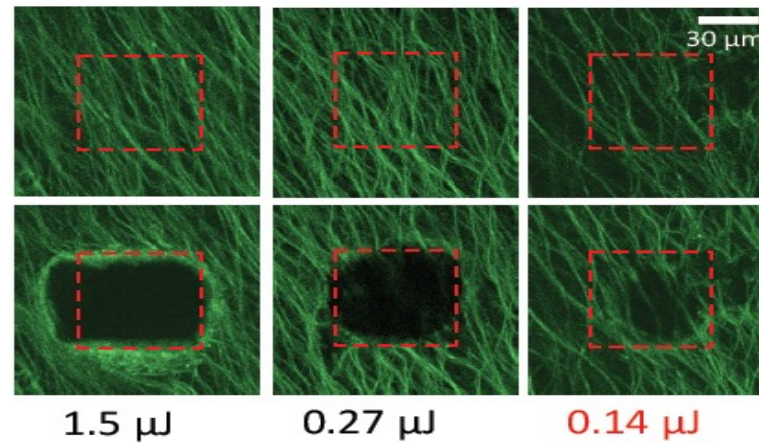
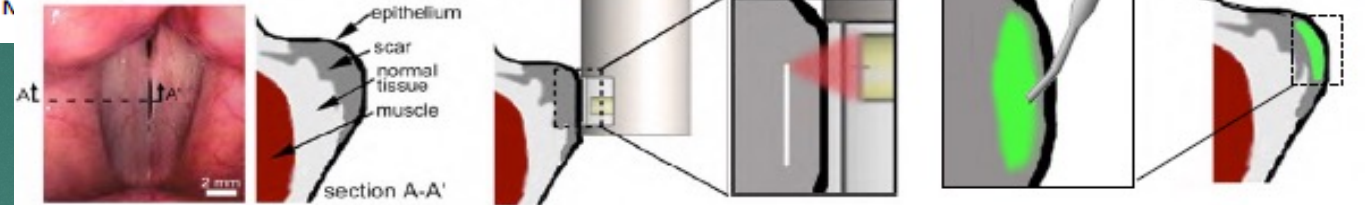
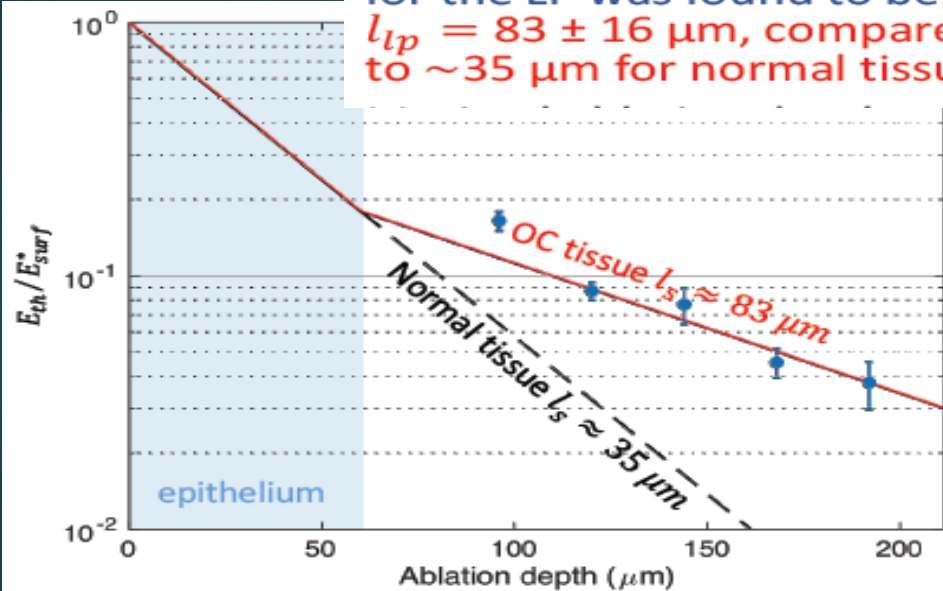
^c Research-Education Institute of Optics and Biophotonics, NG Chernyshevsky Saratov National Research State University, Russian Federation

^d Interdisciplinary Laboratory of Biophotonics, Tomsk National Research State University, Russian Federation

^e Laboratory of Laser Diagnostics of Technical and Living Systems, Institute of Precise Machine Engineering, Russian Federation



The resulting scattering length for the LP was found to be $l_{lp} = 83 \pm 16 \mu\text{m}$, compared to $\sim 35 \mu\text{m}$ for normal tissue



Ablation at threshold fluence (2P imaging)

- $1/e^2$ spot radius $0.7 \mu\text{m}$
- Scanning over the ablation FOV marked in red
- Ablation at $1/15 \text{ fps}$
- **Threshold fluence $\sim 2 \text{ J/cm}^2$**

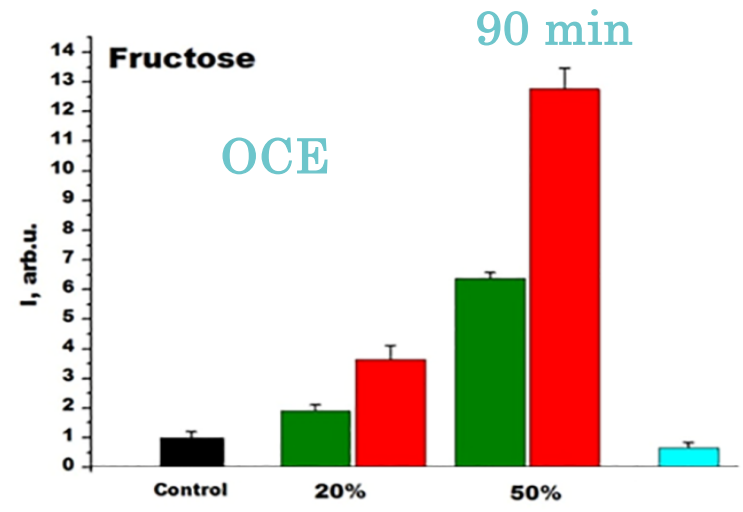
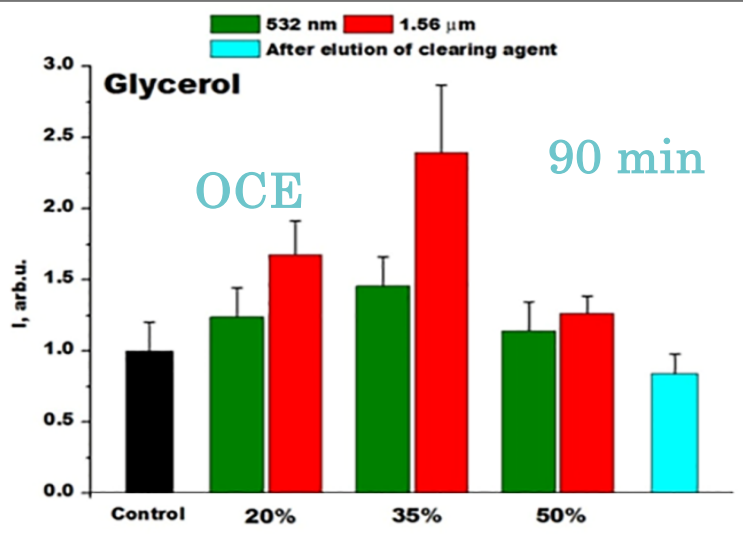
- ❖ **Scarred Vocal Fold** affecting 2-6 M Americans
- ❖ Overuse Surgery Scar affect **the elasticity** of the collagenous layer – Lamina Propria (LP)
- ❖ The scar might extend hundreds of microns deep
- ❖ Treatment: Injection of biomaterial to subsurface voids created by ultrashort laser pulses

Laser treatment of porcine costal cartilage doped by MNPs at OC

Erbium-doped glass fibre laser (IPG Photonics, USA), $d=600 \mu\text{m}$, CW: **1.56 μm** - 5.5 W/cm^2
532 nm - 0.15 W/cm^2

Kinetics of temperature rise

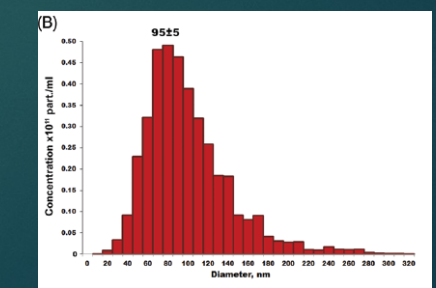
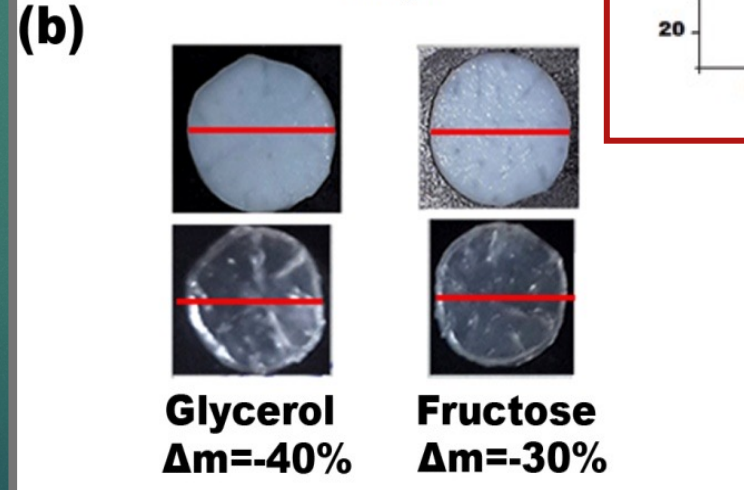
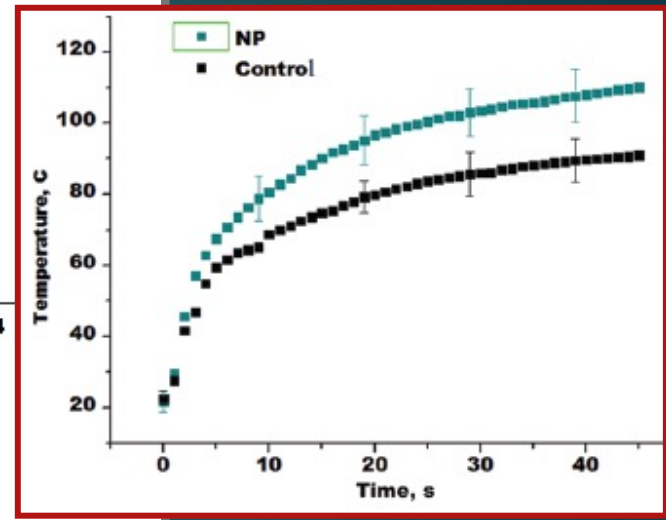
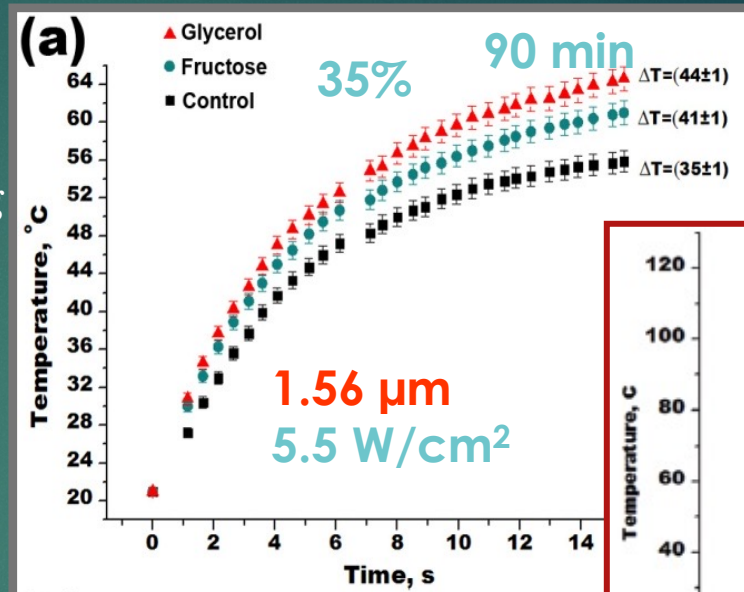
MNPs



❖ OC for $\lambda = 532$ & $1.56 \mu\text{m}$ by applying OCA with different wt% concentrations

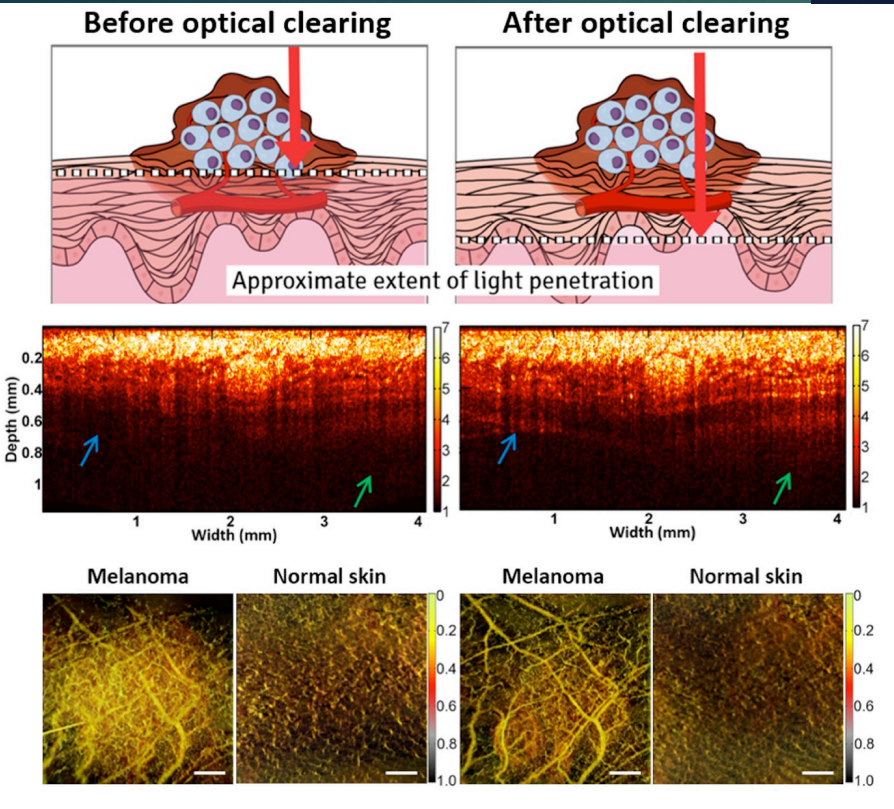
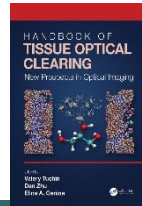
❖ OC efficiency after 10 s from the start of irradiation

❖ Cartilage sample thickness is 1 mm



The role of optical clearing to enhance the applications of in vivo OCT and photodynamic therapy: Towards PDT of pigmented melanomas and beyond

Layla Pires, Michelle Barreto Requena, Valentin Demidov, Ana Gabriela Salvio, I. Alex Vitkin, Brian C. Wilson, and Cristina Kurachi

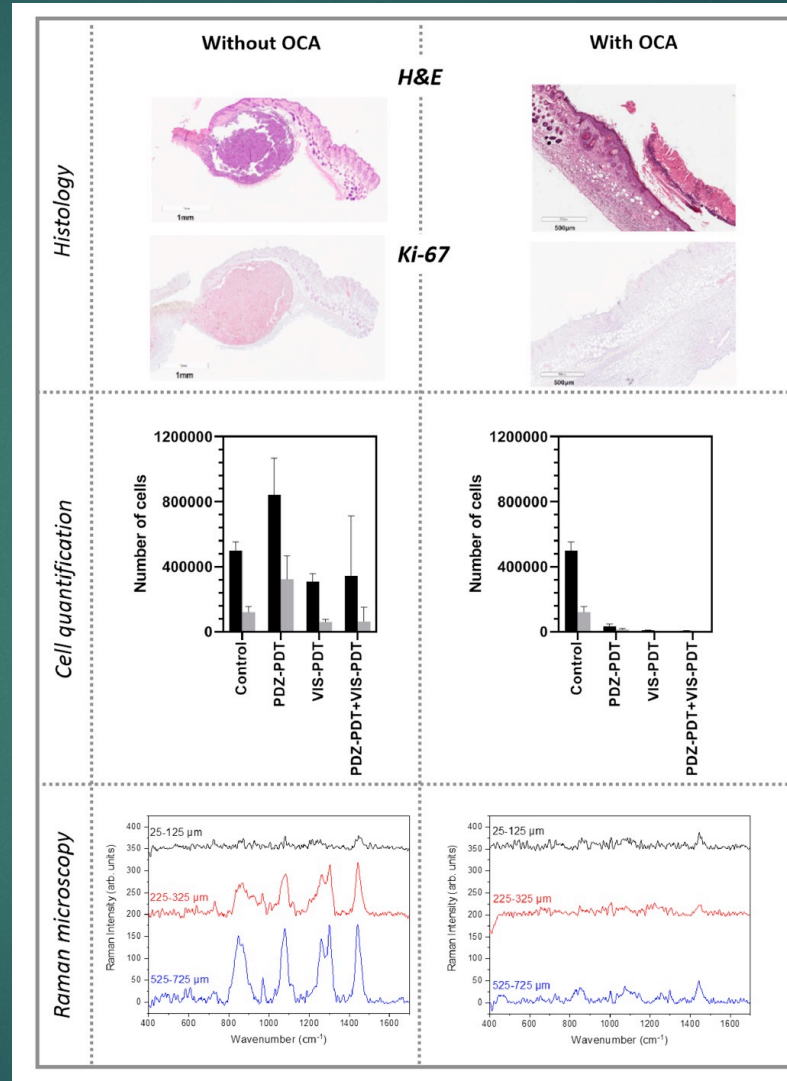


OCT imaging of melanoma before and after OC ($t = 4$ h). Murine B16- F10 tumors in nude mice. Tissue microvasculature images were obtained in speckle-variance OCT (green = top tissue layers, black = deepest). Scale bars are 1 mm.

L. Pires, *et al.*, *Cancers* 12(7), 1956 (2020).

L.P. Martinelli, *et al.*, *Biomedical Optics Express* 11(11), 6516–6527 (2020).

The effect of OC on the PDT outcome in melanotic melanoma



Top row: Histology images (H&E and Ki-67 marker staining viable melanoma cells).

Middle row: Tumor cell counts at $t = 10$ days post-PDT using either the single vascular-targeted photosensitizer Visudyne (VIZ) or tumor cell-targeted photosensitizer Photodithazine (PDZ) or both (means \pm SD: $n = 12$).

Bottom row: Raman microspectroscopy shows that PDZ-mediated PDT damaged the tumor up to $\sim 125 \mu\text{m}$ depth as with OC PDT effectiveness of up to $\sim 700 \mu\text{m}$ depth is observed.

Overview of effects of *in vivo* skin optical clearing on light-induced therapy

JBO Journal of Biomedical Optics

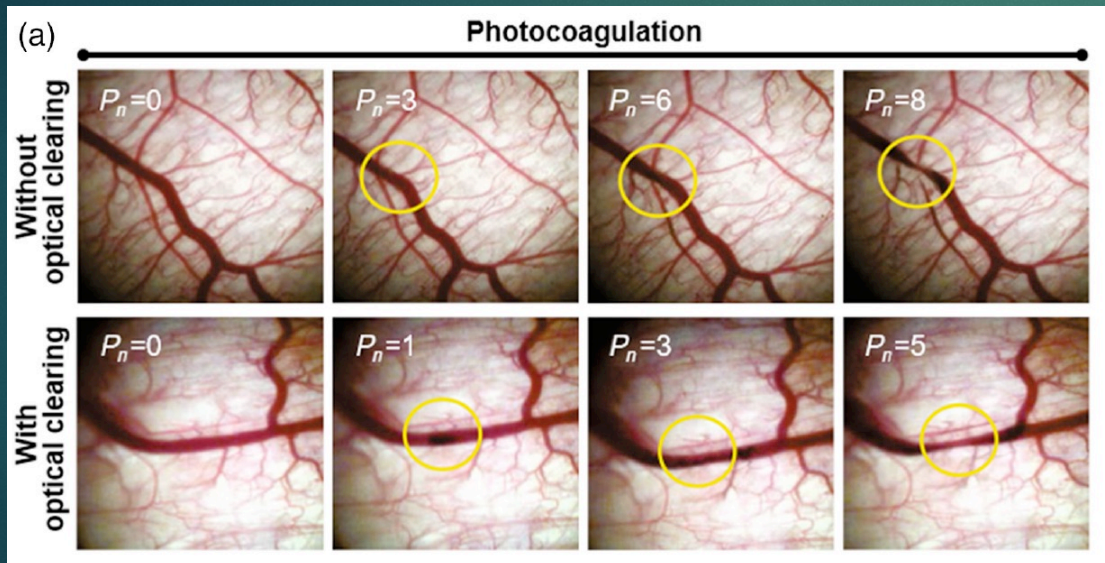
Published June 6, 2023

REVIEW

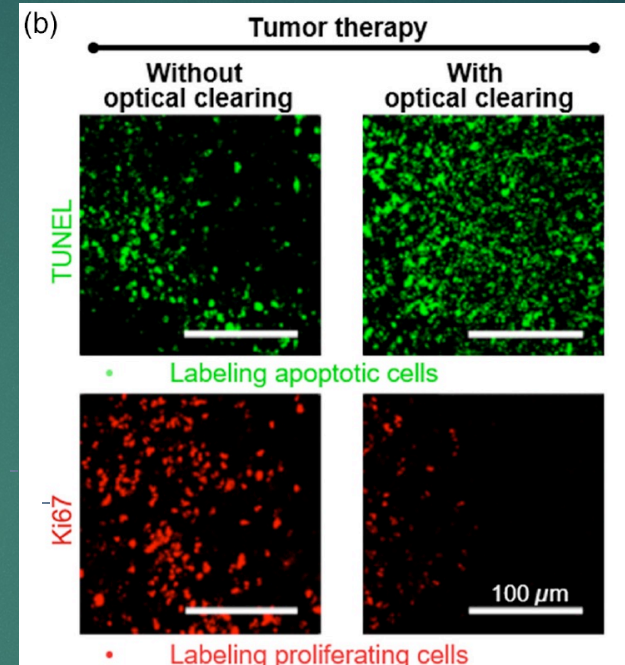
In vivo skin optical clearing for improving imaging and light-induced therapy: a review

Qing Xia,^a Dongyu Li,^{b,*} Tingting Yu,^a Jingtian Zhu,^a and Dan Zhu^{a,*}

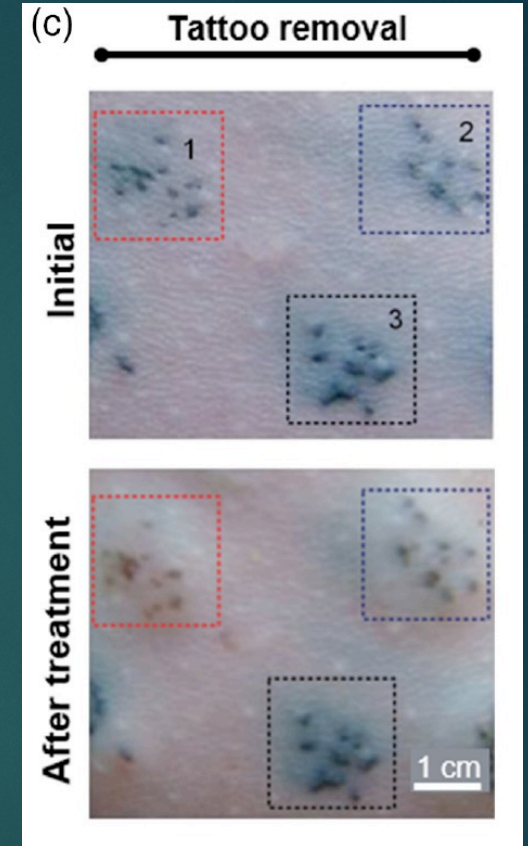
^aHuazhong University of Science and Technology, Britton Chance Center for Biomedical Photonics – MoE Key



(a) Thermal response of blood vessels without or with optical clearing when irradiated with different numbers of laser pulses



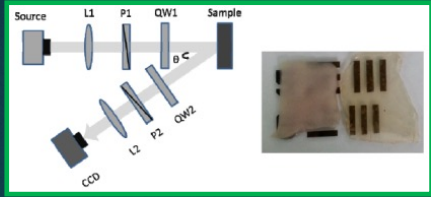
(b) Fluorescence images of TUNEL- and Ki67-labeled tumor slices obtained 14 days after synergistic treatment of **photothermo-chemotherapy** in a deep-seated tumor model without or with OC



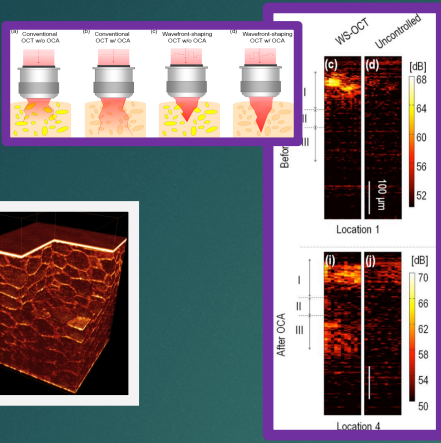
(c) Three pigmentation areas on rat dorsal skin before and after treatments:
area 1: laser irradiation after OC
area 2: only laser irradiation
area 3: without treatment

Summary

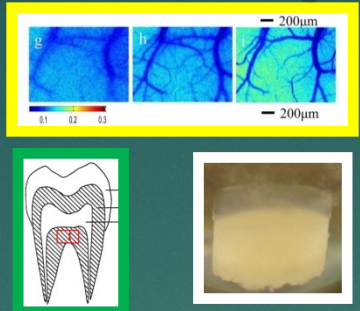
Polarization



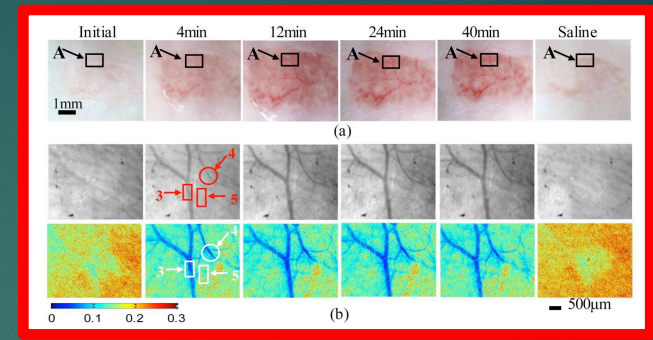
Adaptive OCT



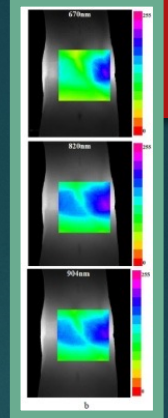
Skull, tooth, bone, cartilage



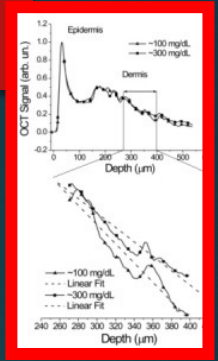
Blood vessel imaging



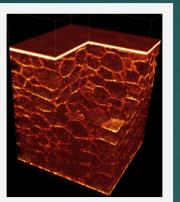
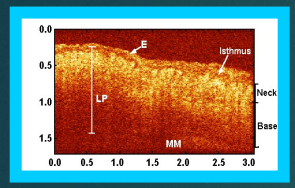
Rheumatoid arthritis



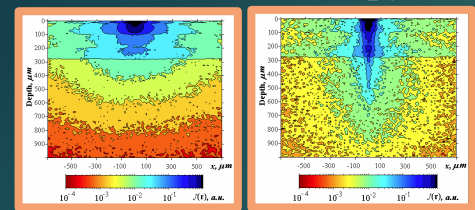
Glucose sensing



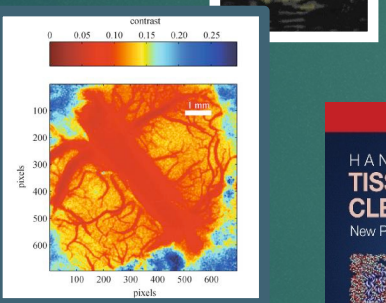
OCT



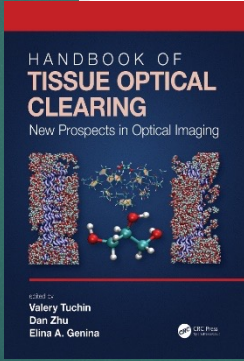
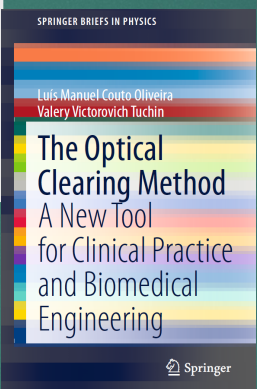
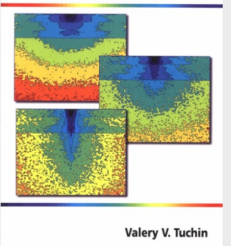
Confocal microscopy



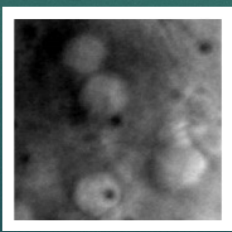
Speckles



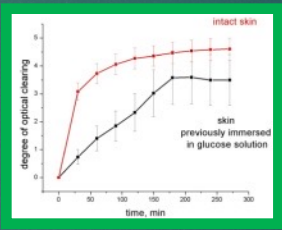
Optical Clearing of Tissues and Blood



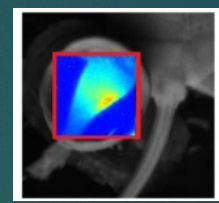
Cell imaging in lymph nodes



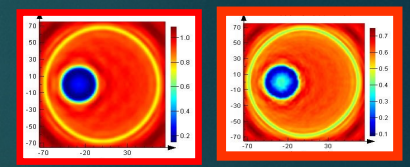
Glycated tissue differentiation



Upconversion nanoparticles

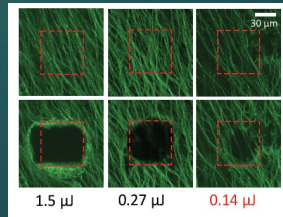


Gold nanoparticles

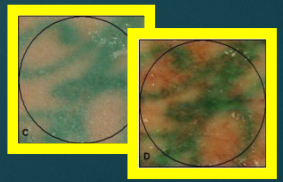


Precise laser surgery

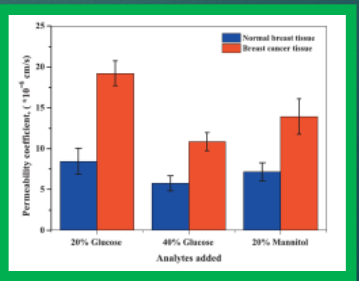
Scarred vocal fold



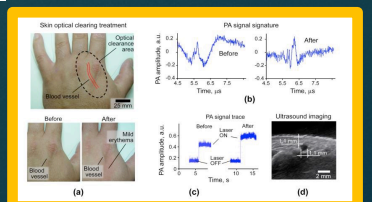
Laser tattoo removal



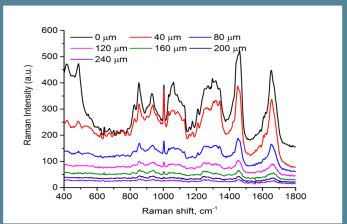
Cancerous tissue differentiation



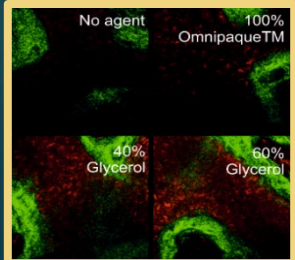
PA microscopy & flow cytometry



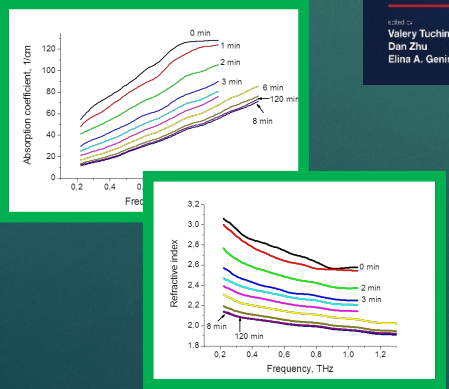
Raman spectroscopy



Two-photon and SHG microscopy



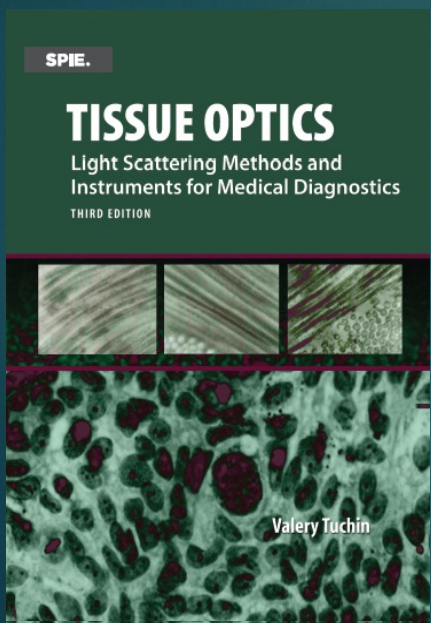
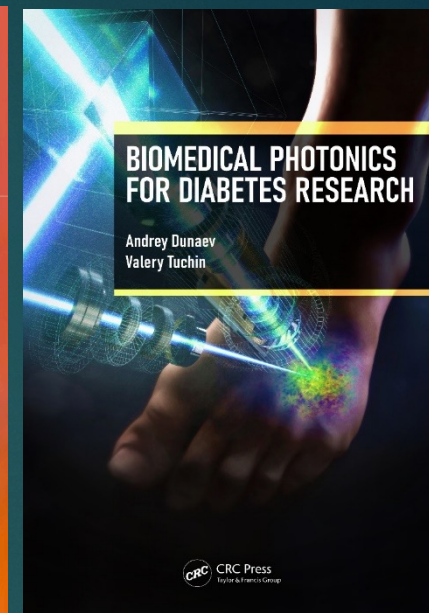
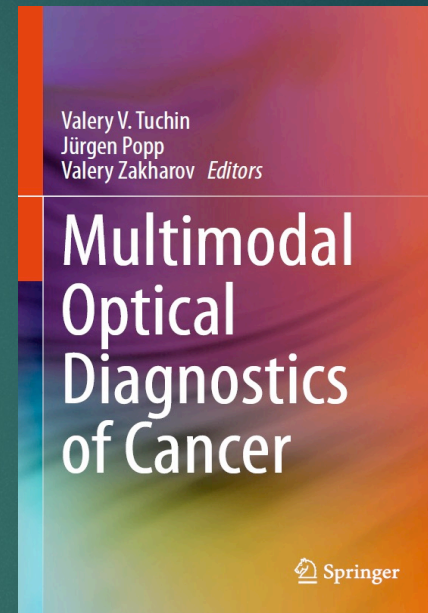
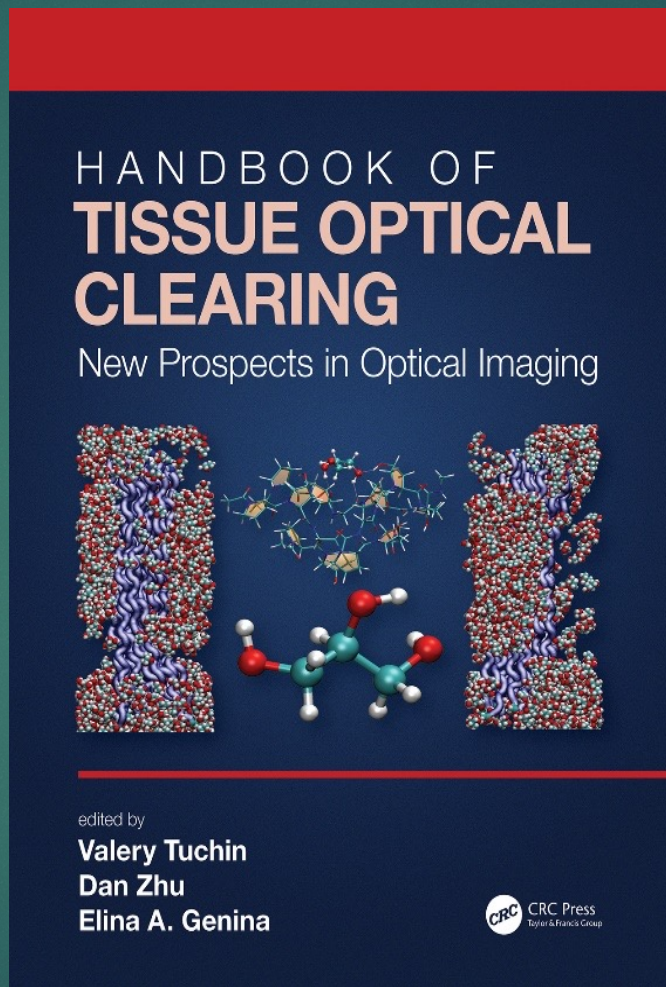
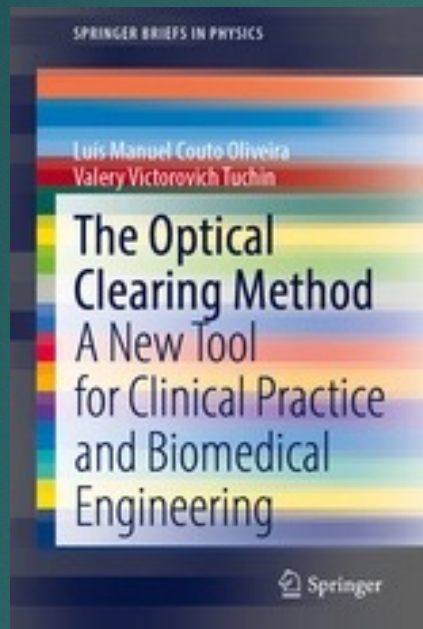
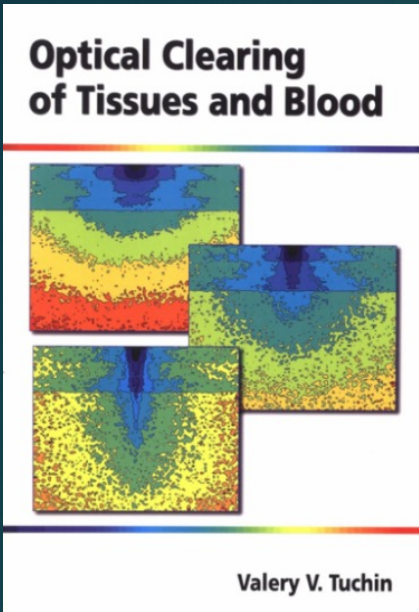
THz clearing



To read:

New book

New book



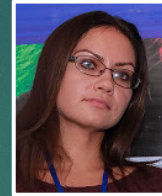
Conclusion

- ❖ Optical clearing technology is beneficial for enhanced multimodal spectroscopy/imaging and PDT/PTT treatment
- ❖ The efficiency of medical lasers working on selected wavelengths in a wide wavelength range from deep-UV to IR range can be improved significantly due to this technology

Acknowledgements

SSU

Elina Genina, Irina Yanina, Polina Dyachenko,
Daria Tuchina, Alexey Selifonov, Vadim Genin,
Ekaterina Lazareva



National and international collaborators

Alla Bucharskaya et al., Saratov State Medical Univer.

Nikolai Khlebtsov et al., Inst. of Biochemistry and Physiology of
Plants and Microorganisms of the RAS

Yulia Alexandrovskaya et al. Inst. Photon Technologies of the RAS

Yury Kistenev, et al. Tomsk State University

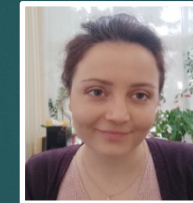
Dan Zhu, Qingming Luo et al. HUST Univ., Hainan Univ. China

Luis Oliveira et al. ISEP-IPP, Porto, Portugal

Alexander P. Savitsky, et al., FRC of Biotechnology, RAS

Alexei A. Bogdanov Jr, UMass, USA

Viacheslav Artyushenko, artphotonics gmbH, Germany



■ Russian Science Foundation grants 23-14-00287

Editorial Board

Editor-In-Chief

Valery V. Tuchin

*Saratov State University,
Institute of Precision Mechanics and Control RAS,
Russia,
University of Oulu, Finland*

Deputy Editor-In-Chief

Valery P. Zakharov

Samara State Aerospace University, Russia

Editorial Board

Stefan Andersson-Engels – Lund University, Sweden
Alexey N. Bashkatov – Saratov State University, Russia
Elina A. Genina – Saratov State University, Russia
Ekaterina Borisova – Academician Emil Djakov Institute of Electronics, Bulgarian Academy of Sciences, Bulgaria
Wei Chen – University of Central Oklahoma, USA
Arthur Chiou – National Yang-Ming University, Taiwan
Min Gu – Swinburne University, Australia
Nikolay G. Khlebtsov - Institute of Biochemistry and Physiology of Plants and Microorganisms RAS, Russia
Juergen Lademann – Charite University Clinic, Germany
Kirill V. Larin - University of Houston, USA
Martin Leahy – University of Galway, Ireland
Qingming Luo – Huazhong University of Science and Technology, China
Stephen J Matcher - University of Sheffield, Great Britain
Igor Meglinski – University of Otago, New Zealand
Vladimir S. Pavlyev - Image Processing Systems Institute RAS, Russia
Francesco Pavone – University of Florence, Italy
Roberto Pini - Institute of Applied Physics, Italy
Igor A. Platonov - Samara State Aerospace University, Russia
Juergen Popp - Institute of Photonic Technology, Germany
Alexander V. Priezzhev – Moscow State University, Russia
David Sampson – The University of Western Australia, Australia
Alexander Savitsky – Institute of Biochemistry RAS, Russia
Alexander P. Shkurinov – Moscow State University, Russia
Peter So – Massachusetts Institute of Technologies, USA
Ilya V. Turchin - Institute of Applied Physics RAS, Russia
Vladimir G. Volostnikov - N.P. Lebedev Physical Institute, Russia
Lihong V. Wang - Washington University, USA
Ruikang Wang - University of Washington, USA
Xunbin Wei - Shanghai Jiao Tong University, China
Dan Zhu - Huazhong University of Science and Technology, China

Welcome to JBPE

I am very pleased to introduce the Journal of Biomedical Photonics & Engineering (JBPE). This new, online-only, open-access journal, published quarterly, is aimed at the rapid dissemination of high-impact results in all areas of biomedical engineering and photonics, from fundamental studies to applied technology.

JBPE will publish original research letters (3-4 pages), research articles (6-12 pages), and reviews (12-20 pages), as well as special issues. All submissions will undergo rigorous reviewing in order to ensure high-quality publications. Papers will be refereed by at least 2 experts as suggested by the Editorial Board. The accepted manuscripts will be published online first in the "Online Ready" section before the whole issue is available.

The Editorial Board is comprised of a fantastic group of renowned researchers and has a diversity of expertise that covers all areas of biophotonics and biomedical engineering. They will work hard to ensure that papers are given careful and quick consideration to maintain the spirit of rapid dissemination.

Starting a journal with such lofty goals is challenging. I am highly encouraged by superb articles that have already been submitted. I wish to express my gratitude to many individuals who have contributed to the successful start-up of the JBPE. I thank all members of the Editorial Board for their efforts in soliciting manuscripts and seeing them through the review process.

Many strategic aspects of JBPE were developed in the course of extensive discussions that I had with many colleagues, and I continue to welcome your thoughts and suggestions on how we can further improve the journal.



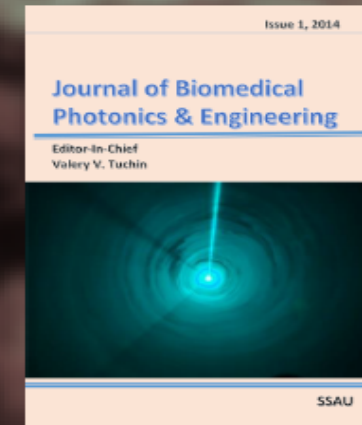
Valery V. Tuchin
Editor-in-Chief

Journal of Biomedical Photonics and Engineering



The Samara State Aerospace University
publishing

presents
an Open Access



**Journal of
Biomedical Photonics
&
Engineering
(JBPE)**



Welcome to SFM-24

September 23 - 27, 2024

<https://sfmconference.org/>

